To the Graduate Council:

I am submitting herewith a thesis written by Jonathan A. Conte entitled "Geochemistry and Tectonic Significance of Amphibolites within the Precambrian Ashe Formation, Northwestern North Carolina". I have examined the final copy of this thesis for form and content and recommend that it be accepted in partial fulfillment of the requirements for the degree of Master of Science, with a major in Geology.

Kula C. Misra

K. C. Misra, Major Professor

We have read this thesis and recommend its acceptance:

Lawrence A. Taylor

Gary G. McSween

Theodore C. Labotka

Accepted for the Council:

Lew Minkel

Vice Provost
and Dean of the Graduate School

STATEMENT OF PERMISSION TO USE

In presenting this thesis in partial fulfillment of the requirements for a Master's degree at The University of Tennessee, Knoxville, I agree that the Library shall make it available to borrowers under rules of the Library. Brief quotations from this thesis are allowable without special permission, provided that accurate acknowledgment of the source is made.

Permission for extensive quotation from or reproduction of this thesis may be granted by my major professor, or in his absence, by the Head of Interlibrary Services when, in the opinion of either, the proposed use of the material is for scholarly purposes. Any copying or use of the material in this thesis for financial gain shall not be allowed without my written permission.

Signature Jonathan A. Conte

Date 2/17/86

GEOCHEMISTRY AND TECTONIC SIGNIFICANCE OF AMPHIBOLITES WITHIN THE PRECAMBRIAN ASHE FORMATION, NORTHWESTERN NORTH CAROLINA

A Thesis

Presented for the

Master of Science

Degree

The University of Tennessee, Knoxville

Jonathan A. Conte

March 1986

DEDICATION

This thesis is dedicated to my parents, Mr. and Mrs. Frank A. Conte

ACKNOWLEDGMENTS

The author acknowledges Dr. K. C. Misra, committee chairman, for suggesting the topic of this study and for his suggestions throughout the manuscript's preparation. Discussions with committee members, Dr. H. Y. McSween, Dr. L. A. Taylor and Dr. T. C. Labotka have also greatly aided in synthesizing data and interpretations. Dr. O. C. Kopp's assistance with x-ray fluorescence apparatus was invaluable. R. McKamey's help with the electron microprobe was also appreciated.

Financial support was provided by The University of Tennessee discretionary fund and by a grant from Sigma Xi.

Immeasurable thanks are also extended to my friends and colleagues in the Department of Geology at The University of Tennessee for their help with this project through informal discussions and also for making my tenure in graduate school as pleasant as possible.

Final thanks go to my parents for their financial and spiritual support.

ABSTRACT

The Late Proterozoic (?) Ashe Formation is a complex assemblage of pelitic schists and gneisses, amphibolites and ultramafic rocks. Although studies of metamorphism of each of these rock types have been conducted, little work has been done to determine the nature of the protoliths for the Formation and the tectonic environment in which the original rocks were deposited. To explore this aspect of the Ashe, a detailed geochemical study of amphibolites within the Ashe and the overlying Alligator Back Formation has been carried out.

Petrographic study of 78 samples, 62 from the Ashe and 16 from the Alligator Back, shows that the assemblages present in amphibolites from the Ashe are (+qtz + plag + Fe-oxide): hnb + ep, hnb + bio + ep, hnb + gar, hnb + bio, hnb + bio + gn, hnb + gar + ep and hnb + gar + cumm. The last assemblage, hnb + cumm + gar, has not been reported for these rocks. Assemblages in the Alligator Back Formation are (+qtz + plag + Fe-oxide): hnb + ep, hnb + bio + ep and hnb + bio + gar.

Whole rock analyses of 74 samples from these formations reveal three distinct rock types. Group 1 contains rocks characterized by relatively high average values of TiO_2 (3.0%), Zr (200 ppm), Y (45 ppm), Nb (22

ppm), P_2O_5 (0.4%) and FeO* (15.8%). Group 3 is characterized by relatively low averave values of TiO_2 (0.5%), Zr (40 ppm), Y (15 ppm), Nb (<4ppm) and P_2O_5 (0.05%). This group also contains high values of CaO (11-15%) and Ni (110 ppm). Group 2 contains the most samples and is characterized by intermediate values of TiO_2 (1.4%), Zr (110 ppm), Y (30 ppm), Nb (10 ppm) and P_2O_5 (0.2%). Spatially group 1 and 2 rocks occur randomly throughout both formations and often are closely associated, whereas group 3 samples are situated only within the Ashe. On the basis of several discrimination diagrams (Ti-Zr-Y, Ti/V, Y/Nb-TiO_2), it is concluded that group 1 rocks were originally continental flood basalts, whereas group 2 rocks are predominantly metamorphosed ocean floor basalts. Rare earth element patterns support these conclusions. Group 3 rocks are problematic in that their trace element abundances suggest they are metmorphosed intrusive rocks, while their Mg/(Mg + Fe) ratios suggest that they are basalts. This group probably represents a protolith of basaltic composition, yet with a high phenocryst/liquid ratio.

This study shows that amphibolites from within the Ashe Formation are much more variable than was previously considered, however, it is possible to constrain the depositionaly setting of the unit to a rifted passive margin containing crust transitional from continental to

oceanic. These data and conclusions are also consistent with chemical data from other ancient and present-day rifts, and also with regional stratigraphy.

TABLE OF CONTENTS

CHAPTER		PAGE
1.	INTRODUCTION	1
	Objectives of Study	1
	Geologic Setting and Previous Work	3
	Methods of Study	9
	Field Relations of Amphibolites	12
2.	PETROLOGY OF THE AMPHIBOLITES	15
	Petrography	15
	Mineral Chemistry	25
3.	GEOCHEMISTRY	31
	Introduction	31
	Protolith	34
	Tectonic Setting	46
4.	DISCUSSION	62
	Element Mobility	62
	Validity of Discrimination Diagrams	67
	Regional Setting	68
5.	CONCLUSIONS	74
REFFERENCES		76
APPENDICES		84
APPENDIX A.	X-ray Fluorescence Procedures	85
APPENDIX B.	Wholerock Analysis of Amphibolites	93
APPENDIX C.	Representative Hornblende Analyses	107
APPENDIX D.	Other Representative Analyses	110
APPENDIX E.	Mineral Assemblages	117
APPENDIX F.	Abbreviations used in text	120
VITA		122

LIST OF TABLES

TABLE PAGE

1. Whole rock analyses of selected amphibolite samples from the Ashe and Alligator Back Formations (oxides in wt%; elements in ppm) 33

2. Summary of inferred protoliths for amphibolites of the Ashe and Alligator Back Formations 60

LIST OF FIGURES

FIGURE PAGE

1. A generalized geologic map of study area for this project and index map showing regional location (after Rankin et al., 1972) 2

2. A map of metamorphic zones of amphibolites within Ashe and Alligator Back Formations (after Abbott and Raymond, 1984) 7

3. A map showing distribution of amphibolite sample locations for this study 11

4. Photomicrographs of amphibolite lithologies from Ashe and Alligator Back Formations 18

5. Nomenclature of amphiboles from this study (after Leake, 1978) 26

6. Al^{vi} versus A-site occupancy for selected hornblende analyses 28

7. X_{Mg} in hornblende versus X_{An} in plagioclase of selected samples 29

8. Niggli 100*mg-c-(al-alk) plot for amphibolites from the Ashe and Alligator Back Formations 35

9. [(Al + Fe + Ti)/3]-K versus [(Al + Fe + Ti)/3]-Na discriminant diagram (after Bard and Moine, 1979) for amphibolites from the Ashe and Alligator Back Formations 36

10. Al + Fe + Ti versus Ca + Mg discriminant diagram (after Bard and Moine, 1979) for amphibolites from the Ashe and Alligator Back Formations 37

11. AFM plot of amphibolites from the Ashe and Alligator Back Formations 39

12. Nb/Y versus $(Zr/P_2O_5)*100$ discrimination diagram (after Floyd and Winchester, 1975) for amphibolites from the Ashe and Alligator Back Formations 40

13. Variation diagrams of selected major element oxides (weight %) and trace elements (ppm) plotted against Zr 42

FIGURE PAGE

14. Ti/100 - Zr - Y*3 discrimination diagram (after Pearce and Cann, 1973) for amphibolites from the Ashe and Alligator Back Formations 47

15. Logarithmic TiO_2 versus Zr and Zr/Y versus Zr discrimination diagrams (after Pearce and Norry, 1979) for amphibolites from the Ashe and Alligator Back Formations 49

16. V versus Ti/1000 discrimination diagram (after Shervais, 1982) for amphibolites from the Ashe and Alligator Back Formations 50

17. TiO2 versus Y/Nb discrimination diagram (after Floyd and Winchester, 1975) for amphibolites from the Ashe and Alligator Back Formations 52

18. Zr/Nb - Y/Nb - Zr/Y discrimination diagram (after Fodor and Vetter, 1984) for amphibolites from the Ashe and Alligator Back Formations 54

19. TiO_2 vs. FeO*/MgO discrimination diagram (after Fodor and Vetter, 1975) for amphibolites from the Ashe and Alligator Back Formations 56

20. Chondrite-normalized REE patterns from selected amphibolites from the Ashe Formation 57

21. Map showing location of samples with respect to geochemistry 59

CHAPTER 1

INTRODUCTION

Objective of Study

During the past two decades the southern Appalachian Blue Ridge Province has been the focus of much structural, stratigraphic, geochemical, geochronological and geophysical work. The Ashe Formation (Figure 1),located within this province and presumed to be Late Proterozoic in age (Rankin, 1970), consists of amphibole schists and gneisses (amphibolites), pelitic schists and gneisses, and ultramafic rocks (Abbott and Raymond, 1984). The Ashe rocks have undergone at least three, and possibly four, deformational events, including amphibolite facies metamorphism (Abbott and Raymond, 1984), that make the interpretation of their tectonic and depositional settings a difficult task. Although petrologic studies of the various lithologies (Swanson and Raymond, 1981; Abbott and Raymond, 1984) have been conducted to determine the metamorphic history of the Ashe, little quantitative work has been carried out to aid in evaluating the tectonic setting of the protolith.

Geochemical studies of basalts and amphibolites have frequently been used in many areas, including the southern Appalachians (Achiabar, 1983; Stowe et al.,

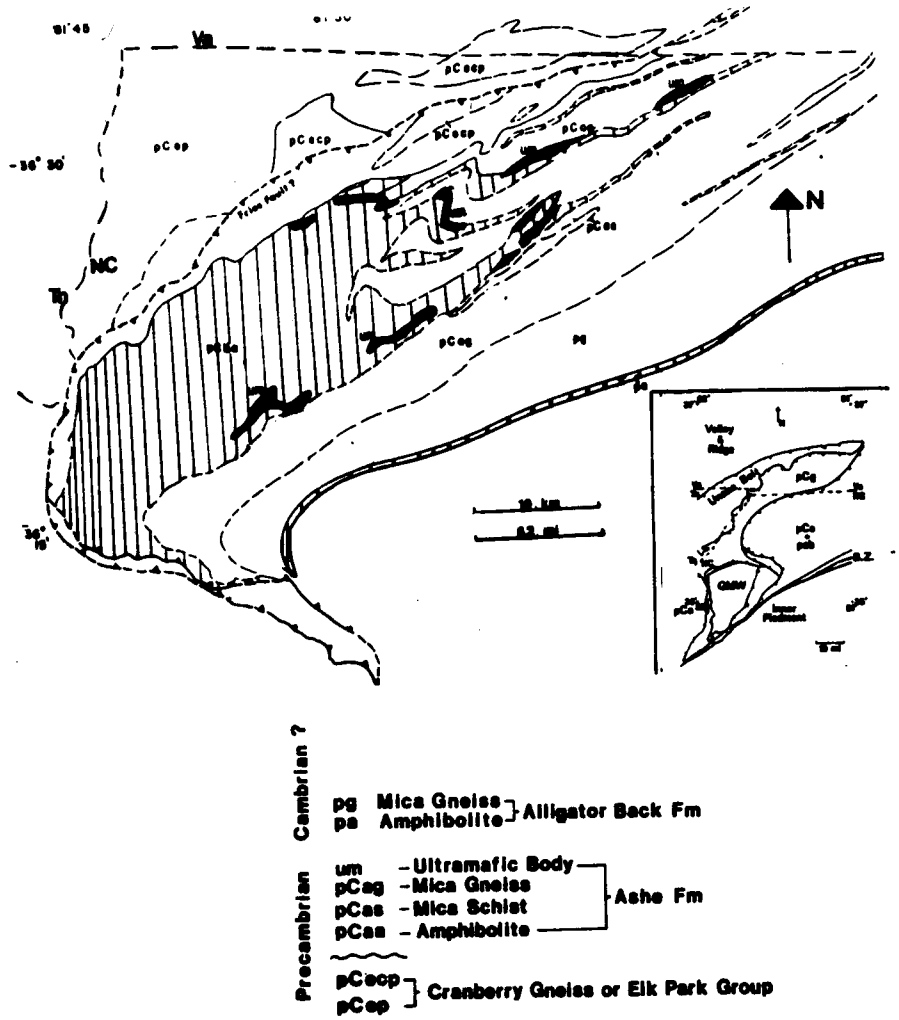

Figure 1. A generalized geologic map of study area for this project and index map showing regional location (after Rankin et al., 1972). Units from which amphibolites were obtained are denoted by vertical lines. For index map: B.Z. = Brevard Zone; G.M.W. = Grandfather Mountain Window; pCa + pCab = Ashe and Alligator Back Formations and pCg = Cranberry Gneiss (Elk Park plutonic group).

1984), to infer the tectonic setting of their protoliths, and a similar study is presented in this report. There are several objectives of this study: (1) to conduct a detailed geochemical study of the amphibolites within a large area of the Ashe Formation and overlying Alligator Back Formation; (2) to use these results to evaluate proposed models for depositional sites of the Ashe; and (3) to use this information to place the Ashe into the regional tectonic framework of the eastern Blue Ridge province.

Geologic Setting and Previous Work

The sections of the Ashe and Alligator Back Formations studied in this project are located within Ashe, Watauga and Wilkes counties in northwestern North Carolina (Figure 1). This area is situated in the Winston-Salem 1° by 2° quadrangle which was mapped by Rankin et al. (1972); the section also includes portions of fifteen $7\frac{1}{2}$ minute quadrangles.

Although the Ashe Formation is composed of many different lithologies, the study area is dominated by amphibolites. Pelitic schists commonly interfinger with amphibolites, especially in the eastern and northern parts of the region, whereas ultramafic rocks are common within the amphibolites (Figure 1). The Ashe extends into southwestern Virginia, where it contains a relative

abundance of pelitic rocks, and south of the Grandfather Mountain window. The Ashe has been correlated with other units in the Appalachian orogen such as the Lynchburg, Mt. Rodgers, Catoctin (Virginia), Tallulah Falls (North Carolina-Georgia) and the Tyson and Houssac Formations (Vermont) (Rankin et al., 1983). Also, Abrams and McConnell (1984) correlated the Ashe with the Sandy Springs and New Georgia Groups in the northern Georgia Piedmont. The total thickness of the Ashe is unknown, but it has been estimated to be at least 15-20 km thick in northwestern North Carolina (Rankin et al., 1972).

The Alligator Back Formation, named by Rankin et al. (1973), conformably overlies the Ashe Formation and is distinguished from the latter in several aspects: (1) the Alligator Back contains less amphibolites and ultramafic rocks; (2) metagreywacke in the Alligator Back Formation is more calcic compared to metagreywacke in the Ashe; (3) the Alligator Back has a unique "pinstriped" appearance. As with the Ashe, the thickness of the Alligator Back is difficult to determine because of intense deformation. It is believed that the Alligator Back Formation is of late Precambrian or early Paleozoic age and may be correlative with the Evington Group of Virginia (Rankin et al., 1983; Wehr and Glover, 1985).

The Ashe Formation in the study area occurs on the southeast flank of the Blue Ridge anticlinorium, a

structure cored by 1 billion year old crystalline rocks. In northwestern North Carolina this group of gneissic rocks is referred to as the Elk Park Plutonic Group (Rankin, 1970). The Eocambrian Crossnore Plutonic suite (820?-680? m.y., Rankin, 1970; Odom and Fullagar, 1984) also occurs within the basement complex. Rankin (1970) and Odom and Fullagar (1984) considered the plutonic rocks of the Crossnore suite to be genetically related to volcanic rocks of the Ashe and Mt. Rodgers Formation; however, it has been reported that the geochemistry of mafic dikes in the basement complex differs significantly from that of the amphibolites in the Ashe (Vincent, 1983).

The nature of the contact between basement rocks (Cranberry Gneiss) and the overlying Ashe is controversial. Based on the occurrence of two outcrops of conglomerate within the Ashe near the contact with the basement, Rankin et al. (1972) concluded that the boundary between the two formations is a nonconformity. On the other hand Abbott and Raymond (1984) contend that the contact is a fault based on the following observations: (1) rocks within the Cranberry Gneiss are of lower grade than rocks directly above the contact with the Ashe; (2) detailed mapping in areas both north and south of the Grandfather Mountain Window indicates that graphitic schists within the Ashe are truncated by the contact; (3) phacoidal blocks of Ashe are incorporated into the

Cranberry Gneiss along shear zones parallel to the contact; (4) ultramafic rocks are much more abundant in the Ashe than in the basement rocks; (5) the units described by Rankin may represent porphyroclastic, mylonitized Cranberry Gneiss rather than basal conglomerates; and (6) there is an apparent lack of a genetic relationship between amphibolites in the Ashe and in the basement. Wehr and Glover (1985) also noted the different depositional environments of late Proterozoic units on either side of the contact (alluvial to shallow marine to the northwest and deep water marine to the southeast).

In the study area Abbott and Raymond (1984) delineated three metamorphic zones of pelitic rocks and two amphibolite zones (zones Im and IIm), with the latter zones being separated by the reaction: Bio + Ep = Hnb + Gn (figure 2). On the basis of reactions in pelitic rocks they concluded that the peak of metamorphism occurred at approximately 700°C and greater than 7 kb pressure. Preliminary investigation of the mineral chemistry (McSween, pers. comm.) suggests similar P-T conditions of metamorphism (T=625°C at an assumed P= 7kb).

Very little has been published on the geochemistry of the Ashe Formation amphibolites. Bryant and Reed (1970) obtained a few whole rock analyses (major oxides) of amphibolites from the Ashe in the vicinity of

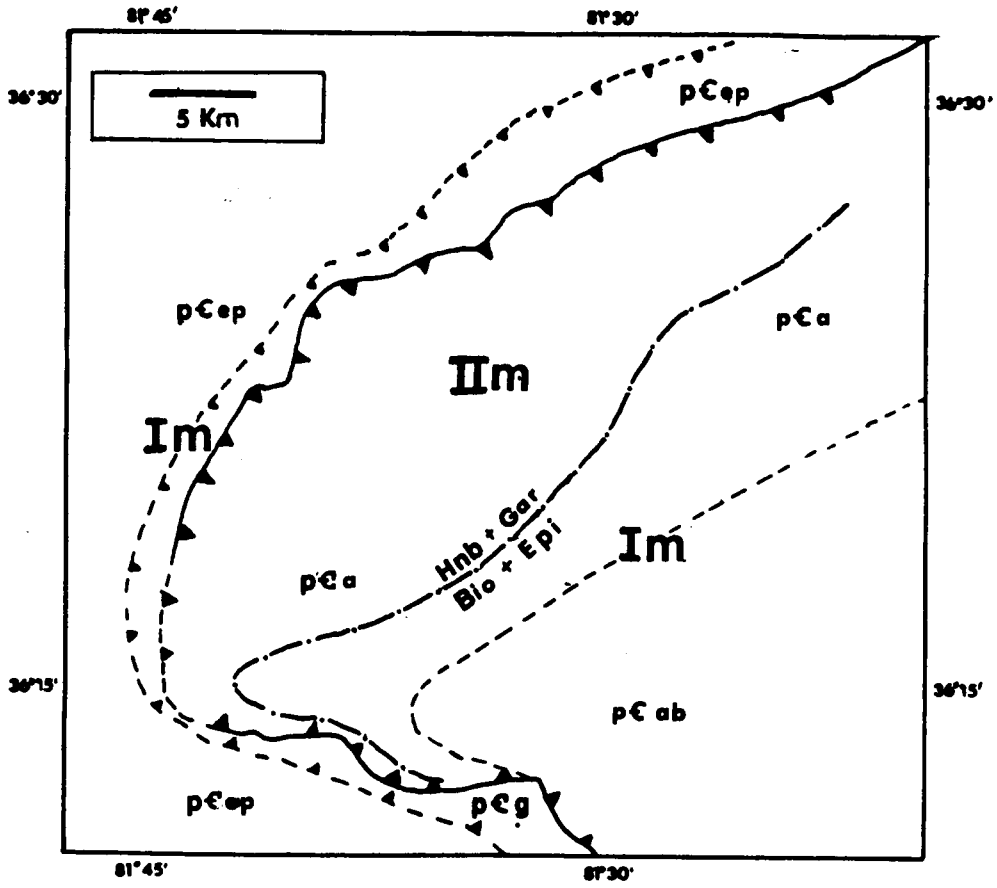

Figure 2. A map of metamorphic zones of amphibolites within Ashe and Alligator Back Formations (after Abbott and Raymond, 1984). Zone IM is of relatively lower grade than zone IIM. Note that Cranberry Gneiss amphibolites are of lower grade than higher grade Ashe amphibolites.

Grandfather Mountain window. From these analyses, they suggested that hornblende schists must have been derived from mafic tuffs or sedimentary rocks, whereas thicker amphibolite layers probably represent mafic flows or sills. Gair and Slack (1984) published a detailed geochemical and mineralogical study of the Ashe Formation associated with the Gossan Lead massive sulfide deposit in southwestern Virginia. These authors examined 15 samples of amphibolites and other mafic rocks and concluded that the protoliths for the samples represent mid-ocean ridge type basalts; one sample from a relatively high stratigraphic position, however, showed characteristics of a continental tholeiite. Gair and Slack also concluded that samples from their study were comagmatic and genetically related.

Several possible tectonic settings have been proposed for deposition of the Ashe, most of which are related to a rifted continental block. Abbott and Raymond (1984) grouped these into four categories: (1) an ensialic, passive margin (Rankin, 1970, 1975; Rankin, Espenshade and Shaw, 1973); (2) a passive, ensimatic or transitional margin; (3) an ensimatic, active margin (Raymond and Swanson, 1981); and (4) a back-arc basin (Stevens, Strong and Kean, 1974). Based on field relations and the known regional history, Abbott and Raymond (1984) favored the second hypothesis. On the

basis of stratigraphic and structural relations, Wehr and Glover (1985) concluded that the Ashe was deposited on attenuated continental crust seaward of a hinge zone represented by the present-day Hayesville-Fries-Rockfish Valley fault. According to this interpretation the Ashe and Alligator Back Formations are vestiges of deep water deposition in this rifted basin.

During deformation subsequent to its deposition, the Ashe was telescoped and transported westward as a massive crystalline thrust sheet into its present position (Hatcher, 1978). COCORP data (Cook et al., 1981) and the presence of autochthonous rocks in the Grandfather Mountain window are compatible with this hypothesis.

Methods of Study

Field work for this project consisted of collecting samples from the study area shown in figure 1 (p. 2). For this study, no detailed mapping was necessary as the reconnaissance mapping by Rankin et al. (1972) proved to be of sufficient accuracy for the present purpose.

Fresh exposures of amphibolites are quite abundant in the area. Most of the Ashe samples were collected from fresh exposures along three transects. Samples in the Alligator Back Formation were collected from the prominent, continuous amphibolite unit mapped by Rankin et

al. (1972). Locations of the samples collected for this study are shown in figure 3.

A total of 116 amphibolite samples, 96 from the Ashe and 20 from the Alligator Back Formation, were collected for this study. Samples were slabbed perpendicular to foliation. From these slabs, 62 polished thin sections of the Ashe and 16 sections of the Alligator Back were prepared for reflected and transmitted light petrographic study.

Preparation for bulk rock analyses by X-ray fluorescence involved crushing chips from selected slabs with a ceramic (Al_2O_3) grinding mill, and making pressed pellets using boric acid as the flux. The constituents analyzed included the elements Si, Al, Ca, Mg, Na, Mn, K, Fe, Ti, P, Cr, V, Ni, Rb, Sr, Y, Zr and Nb. Analyses of 74 samples were performed with an EG & G ORTEC X-ray fluorescence spectrometer. The system has been calibrated for igneous rocks using 22 reference materials and selected analyses of standards are given in Appendix A. Rare earth elements were analyzed commercially by Nuclear Activation Services, Ann Arbor, Michigan, using neutron activation. Normative and Niggli calculations were computed assuming Fe^{2+}/Fe^{3+} ratios for average amphibolites (0.71, McElhaney, 1983).

Using the whole rock geochemistry as a guide, mineral chemistry was analyzed in phases from four samples

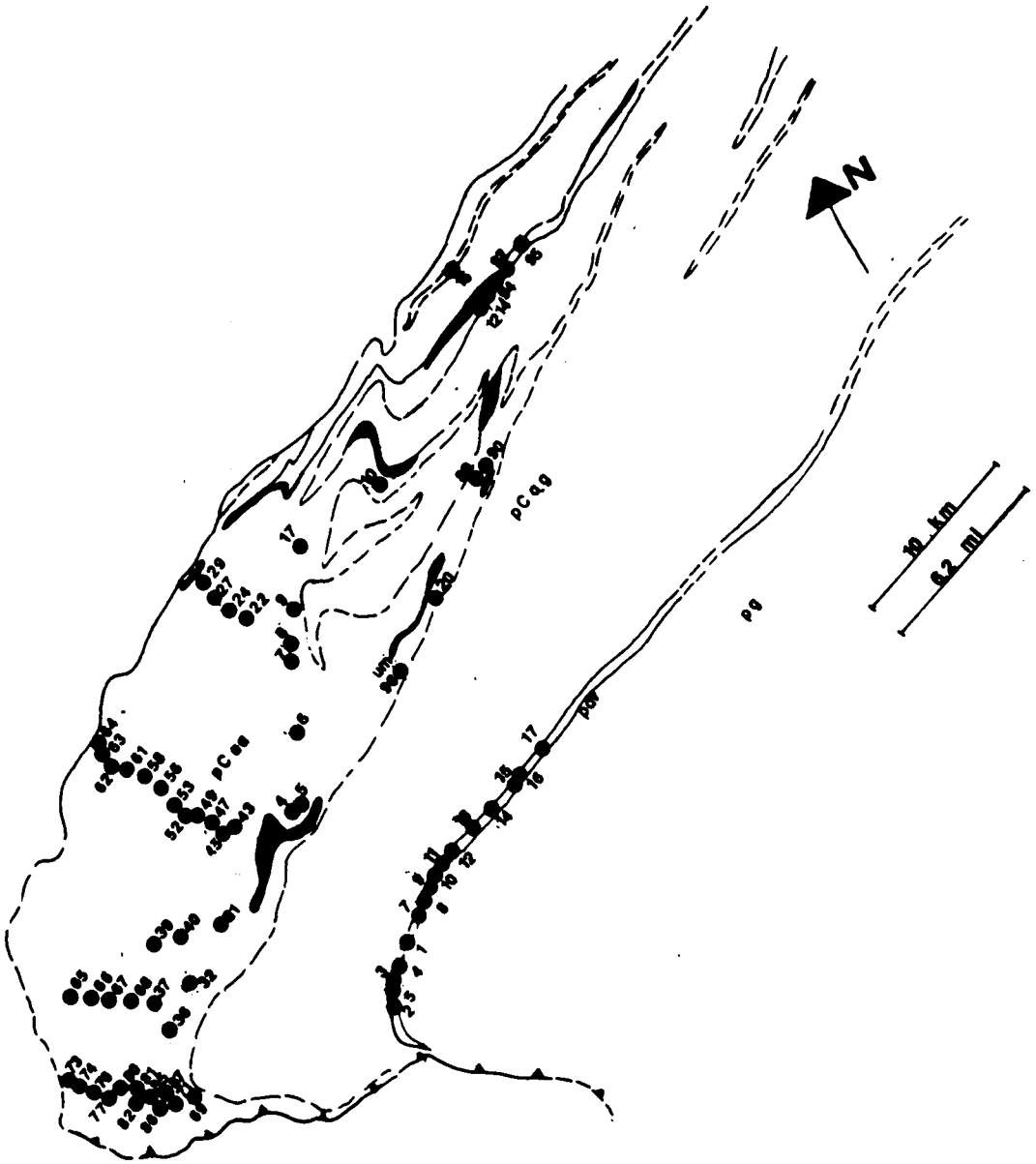

Figure 3. A map showing distribution of amphibolite sample locations for this study. Formation abbreviations are the same as in figure 1.

using an automated MAC 400S electron microprobe. During analyses the accelerating voltage was 15 kV. A beam current of 0.03 μA and defocused beam were used for plagioclase analyses, whereas a current of 0.05 μA was used for hornblende, garnet, ilmenite, cummingtonite, biotite and epidote. The microprobe data were reduced using the correction procedure of Bence and Albee (1968) and Albee and Ray (1970).

In each thin section four to six grains of each phase were analyzed, with three to five analyses being performed on each grain. Average values and standard deviations were then calculated. Amphibole analyses were recalculated by normalizing to 15 cations (less K + Na or less K), 13 cations (less Ca + Na + K) (Robinson et al., 1982) and to 23 anions.

Field Relations of Amphibolites

Exposed amphibolites in the Ashe Formation are generally massive units. Contacts of amphibolites with adjacent units (amphibolites, pelitic units or ultramafic bodies) are rarely visible. Where the contacts between mafic and pelitic units are observed (e.g. intersection of U. S. 221 and N.C. 194 near Baldwin), they are sharp and parallel to the general regional foliation (dipping approximately 40° SE). At that locality several

interfingering units of mafic and felsic affinity are observed.

Several generations of folding are visible in non-amphibolitic units in some areas. Three foliations are commonly seen in the units as described by Jones (1976), who also observed the rare presence of a fourth foliation in rocks near the crest of Mt. Jefferson (Jefferson Quadrangle). Microscopic folds are rare within the mafic units, but folds are sometimes visible on outcrop scale in these units (e.g. at quarry on highway N.C. 113 approximately 1.2 km. west of intersection with U.S. 221).

Within the mafic units the most common and most variable features are felsic bands of plagioclase and quartz and, rarely, of plagioclase, quartz and calcite. The bands range from less than 1 cm to 15-20 cm in thickness. These bands appear to have formed by metamorphic segregation processes.

Field relations do not provide unequivocal evidence for determination of the protolith of the amphibolites. For example it is possible that the banding in some of the amphibolites may represent primary sedimentary layering. In a regional sense the massive nature of the amphibolite suggests that the protolith was originally a thick agglomeration of extrusive mafic rock. Previous chemical analyses (Bryant and Reed, 1970) suggest a protolith of

tholeiitic basalt, but that conclusion is based only upon major element compositions of very few samples from a large area. This is one of the questions examined in the present study.

CHAPTER 2

PETROLOGY OF THE AMPHIBOLITES

Petrography

Amphibolite samples from the Ashe and Alligator Back Formations may be divided into two petrographic groups: samples with a strong foliation formed by the parallel alignment of hornblende and samples that show a less well developed, or no distinct foliation. The division of these two groups is generally a function of either the grain size of hornblende or the relative proportions of hornblende and plagioclase. Hornblende grain sizes throughout the samples are quite variable, ranging from approximately .1 mm to 6.0 mm. Often samples with coarse-grained (>2 mm) hornblende display no strongly developed foliations, whereas samples with fine-grained hornblende are nematoblastic. Compositional layering occurs in many samples and is manifested by hornblende-rich layers alternating with layers rich in plagioclase, quartz and in some cases, epidote. In all the amphibolites hornblende and plagioclase are typically the predominant minerals with hornblende usually comprising approximately 50-70% of a given sample. Other minerals present are quartz, garnet, epidote, clinozoisite, biotite, ilmenite, cummingtonite, chlorite,

sphene, rutile, magnetite, iron sulfides, zircon and apatite.

The assemblages observed in Ashe amphibolites in this study are (+quartz + plag + Fe-oxide):

hnb + bio + ep,

hnb + ep,

hnb + gar,

hnb + bio,

hnb + bio + gar,

hnb + gar + ep,

hnb + gar + cumm.

With the exception of the assemblage hnb + gar + cumm, the rest of these assemblages were observed by Abbott and Raymond (1984) in their detailed petrologic study of the Ashe. They also noted the presence of the assemblage bio + gar + ep. Assemblages in the observed Alligator Back Formation amphibolites are hnb + ep, hnb + ep + chl, hnb + bio + ep, and hnb + bio + gar. The last assemnblage is seen only in one sample (AB-1); hnb + ep is the most common assemblage in the Alligator Back amphibolites. Equilibrium among the coexisting phases is often suggested in thin section by straight, sharp grain boundaries and the absence of secondary reaction products. Chlorite, however, is formed occasionally as a retrograde product replacing hornblende.

Hornblende in samples from this study displays a wide range of textures. Granoblastic hornblende (figure 4A) displays polygonal boundaries with other amphiboles, biotite, garnet, quartz and plagioclase. Inclusions of quartz and plagioclase are ubiquitous; inclusions of apatite, sphene and rutile are quite common. Some of the hornblende is characterized by irregular, ragged crystal faces (AB-2). Generally this type of hornblende is relatively fine-grained. Pleochroism in hornblende is quite variable, but the most common color schemes are green to yellow-green to pale yellow, blue-green to lime green, and pale green to yellow-brown. Hornblende from amphibolites in the Alligator Back Formation is similar to that in the Ashe; however, in the Alligator Back the fine-grained variety occurs much more commonly than the coarse- grained type.

Plagioclase occurs in many forms, the most common of which is represented by clear, tabular grains either situated between larger grains of hornblende or coexisting with quartz in layers free of hornblende. Plagioclase is rarely larger than the average hornblende grain for a given sample, although in some cases the feldspar occurs as large, twinned crystals with inclusions of hornblende (As-37). Most plagioclase is clear, although two samples from the Alligator Back Formation (AB-15, AB-16). show partial sericitization. Twinning is common and several

Figure 4. Photomicrographs of amphibolite lithologies from Ashe and Alligator Back Formations: (A) Granoblastic hornblende (As-85); crossed nicols; (B) Idioblastic garnet with hornblende and plagioclase (As-67); plane light; (C) Idioblastic epidote with hornblende (AB-15); crossed nicols; (D) Symplectic epidote-plagioclase intergrowth (As-86); crossed nicols; (E) Biotite crossing predominant hornblende foliation (As-8); crossed nicols; (F) Chlorite replacing hornblende (AB-5); crossed nicols; (G) Aggregates of ilmenite occurring with finer grained hornblende and plagioclase (As-14); crossed nicols. Scale bar is 0.5 mm.

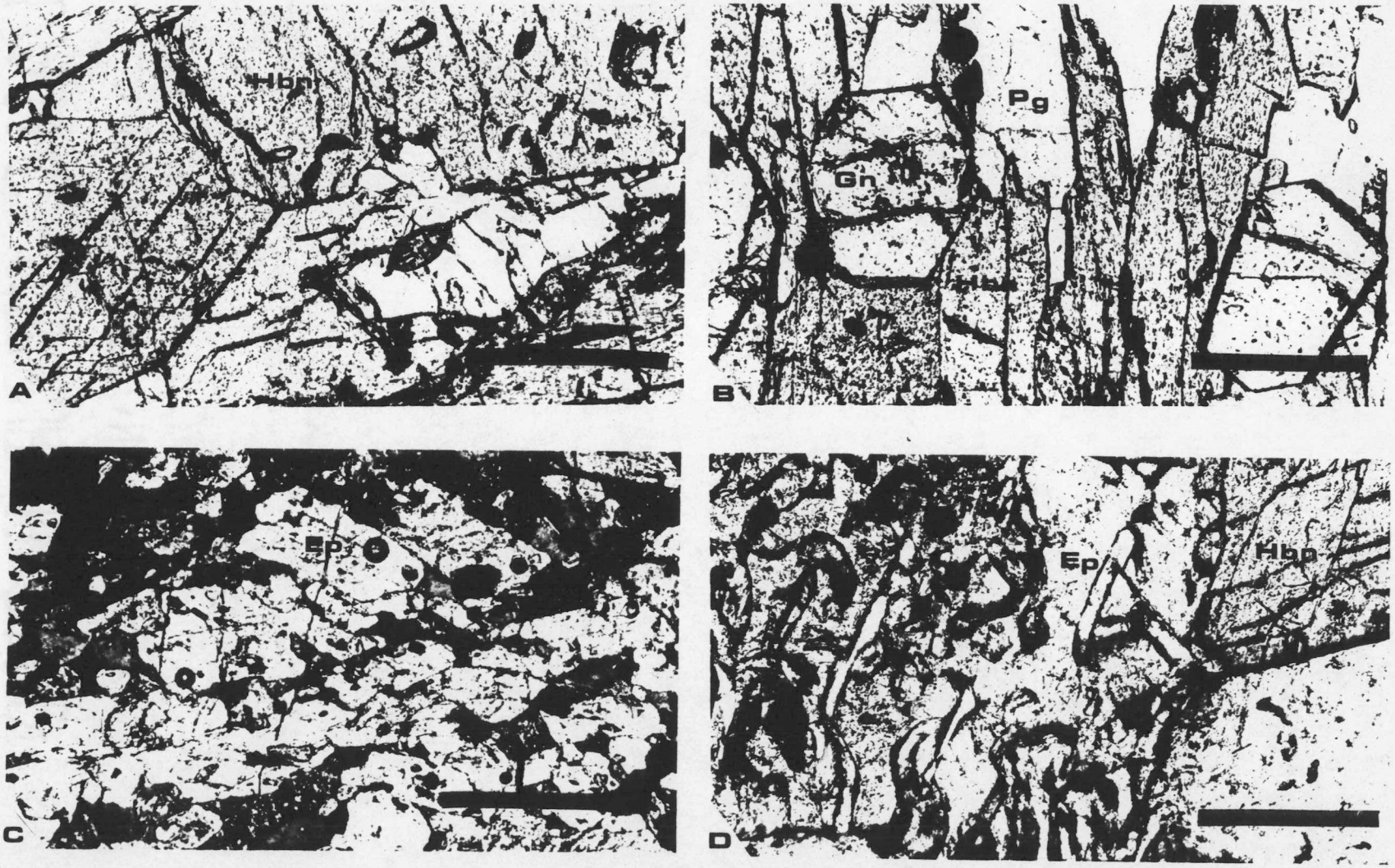
Hbn
A
Pg
Gn
B
Ep
C
Ep
Hbp
D

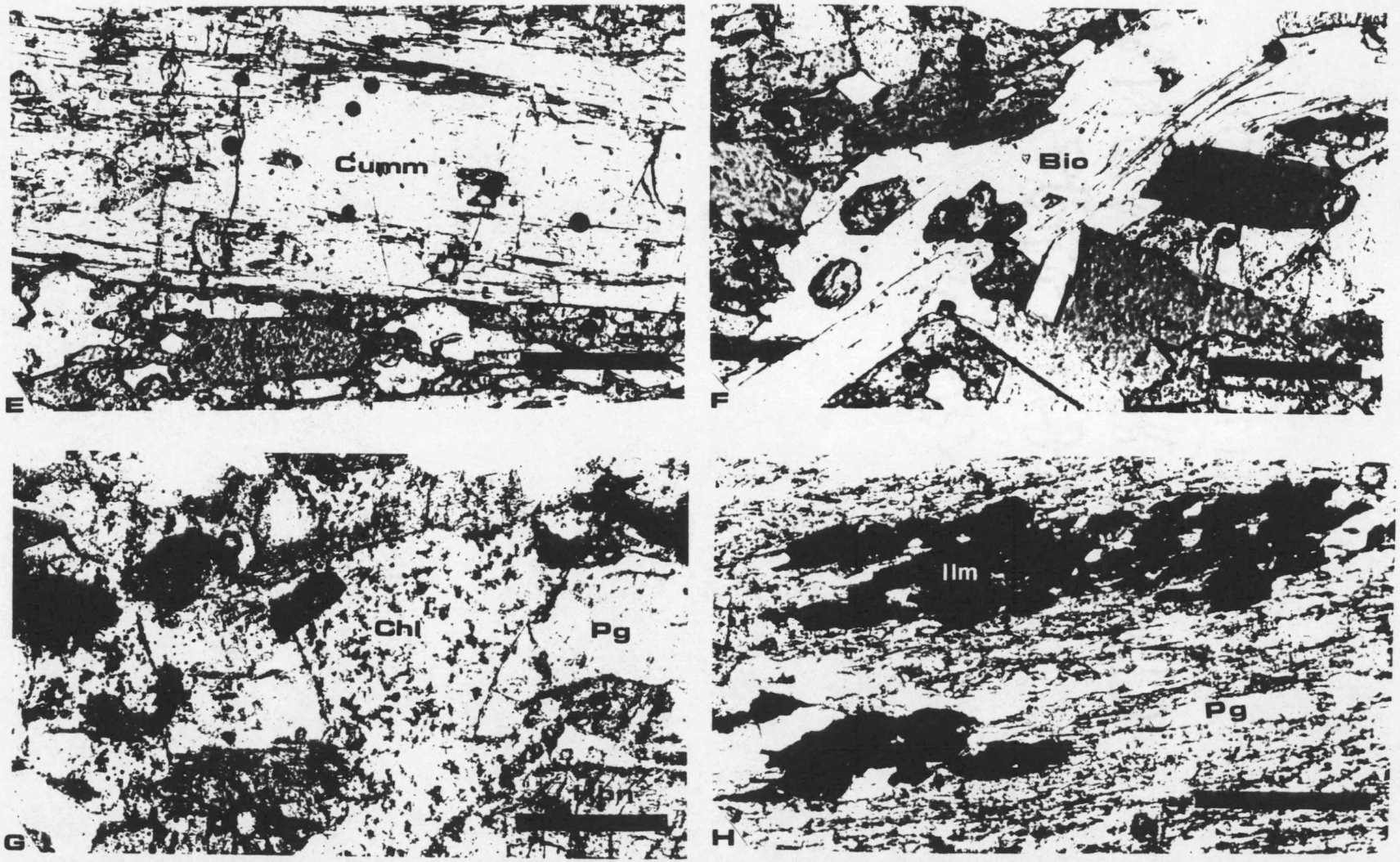
Cumm
E
Bio
F
Chl
Pg
G
Ilm
Pg
H

types occur, the most common of which are the albite and pericline varieties. Zoned plagioclase is uncommon. Except for rare sericitization observed in samples AB-15 and AB-16, plagioclase in the Alligator Back has characteristics similar to those of plagioclase in the Ashe.

Quartz is present typically as small (<.4 mm), xenoblastic grains that occur either between larger grains of hornblende, as inclusions in hornblende and/or garnet, or with plagioclase as bands segregated from hornblende-rich layers. Within the quartz-plagioclase layers, the two components are often recrystallized so that "triple junction" boundaries are common.

Garnet occurs in several samples and ranges in diameter from approximately .25 mm to 5 mm. In general the shapes of the garnets are dependent on grain size; i.e. larger grains have ragged crystal faces, whereas relatively small grains are idioblastic (figure 4B). Garnet commonly contains several types of inclusions, especially plagioclase, quartz and ilmenite. These inclusions, however, show no internal fabric such as helicitic or "snowball" textures. The modal percentage is approximately 10-15% in most samples, whereas two samples, As-4 and As-77, contain approximately 30%. Garnet is present in only one sample from the Alligator Back Formation (AB-1). In this sample, garnets are large

(approximately 3.5 mm in diameter), idioblastic and often are adjacent to biotite grains.

Epidote occurs in many samples from both formations and is present in several forms. The most common type is represented by small, yellow idioblastic grains approximately 1 mm in length which are associated with both hornblende-rich and plagioclase-rich layers (figure 4C). The latter type is especially common in the Alligator Back Formation. A second type of epidote is represented by large (8 mm) porphyroblasts associated with layers of quartz and plagioclase (As-53). These pophyroblasts are poikilitic, containing inclusions of quartz, plagioclase and epidote. Another type of epidote is texturally unique; this form consists of intergrown quartz, plagioclase and epidote resulting in a symplectic texture (As-86) (figure 4D). Such texture was also described by McElhaney (1983) and was interpreted as a product of retrograde metamorphism.

Cummingtonite occurs in one sample (As-22) (figure 4E). It is present as elongated prisms ranging in length from <1 mm to 5.5 mm and is parallel to the foliation defined by more common hornblende.

Biotite occurs in only four samples from the Ashe Formation and one from the Alligator Back. It exists mainly as long (1-2 mm) plates that define a weak foliation different from the predominant one (As-8)

(figure 4F), or it may be parallel to the major foliation. Pleochroism ranges either from pale yellow to red-brown or brown to yellow-brown. Biotite generally possesses straight boundaries with adjacent minerals. This is especially evident in sample AB-1.

Chlorite is present in several samples from the Ashe Formation, but is apparently always the product of retrograde metamorphism. It generally replaces or forms at the boundaries of hornblende, but pseudomorphs after biotite are also observed (As-8). The chlorite usually displays a pale green color in plane light and grey-black interference colors indicating that the mineral may be Mg-rich.

Chlorite is common and is also an alteration product within the Alligator Back Formation. Textures of the mineral are variable, usually occurring as either small plates or radiating aggregates. Examples of the latter texture are particularly evident in AB-5 (figure 4G). Chlorite in the Alligator Back Formation differs from chlorite in the Ashe in that the former displays a deeper green color in plane light and commonly has anomalous (blue, blue-purple) interference colors. This indicates a composition relatively richer in Fe. Chlorite usually forms at the expense of hornblende in this unit.

Sphene is present in many samples within the Ashe Formation, but is absent in the Alligator Back. The

mineral generally occurs as small (<.5 mm in length), wedge-shaped grains randomly distributed throughout the sample. In one sample (As-36), however, sphene is associated with ilmenite and the two often form short trains parallel to the overall foliation. The association of sphene and ilmenite is not uncommon in amphibolites and has been interpreted by Spear (1981) to represent a reaction relationship between the two as a product of retrograde metamorphism. Another common feature of sphene is the inclusion of small grains of rutile.

Ilmenite is the most common opaque phase in the Alligator Back Formation. It occurs in amounts ranging from traces to approximately 10-12%. Its textures are quite variable; those commonly observed are: isolated, amorphous grains randomly distributed throughout, inclusions in larger garnet and hornblende grains, and irregular aggregates aligned parallel to foliation (figure 4H). In the latter type grains often display straight "triple junction" boundaries. Hematite intergrowths are rare but they do occur. These intergrowths are present as thick lamellae or foliated blebs.

Along with ilmenite several opaque phases occur, none of which exceeds 1-2% of a given sample. These minerals include (in order of decreasing abundance) magnetite, chalcopyrite, pyrrhotite and pyrite. All phases are randomly distributed throughout a given sample.

Mineral Chemistry

Although the focus of this study is the whole rock geochemistry of the Ashe and Alligator Back Formations, mineral chemistry of 4 samples representative of different chemical composition were determined. These samples were chosen on the basis of differing chemical compositions, assemblage variance and presence in different formations. Analyzed phases include hornblende, plagioclase, ilmenite, cummingtonite, garnet, biotite and epidote. Representative analyses are given in appendices C and D. It should be noted that these analyses were not carried out with the intent of quantitatively determining pressure and temperature constraints on the Ashe Formation, as these parameters are being evaluated by McSween and Abbott (in prep.).

Hornblende grains analyzed by the microprobe are all calcic (appendix C), with $(Ca + Na)_B > 1.34$, and are plotted on figure 5 (after Leake, 1978). Using this monemclature, most hornblende grains may be classified as tschermakitic or ferroan pargasitic hornblende. One analysis from AB-15 is somewhat anomalous in that its relatively high Si content places it in the actinolitic hornblende field. This sample is also the only one analyzed which showed appreciable zonation. A plot of Al^{VI} vs. A-site occupancy (Figure 6) shows the possible

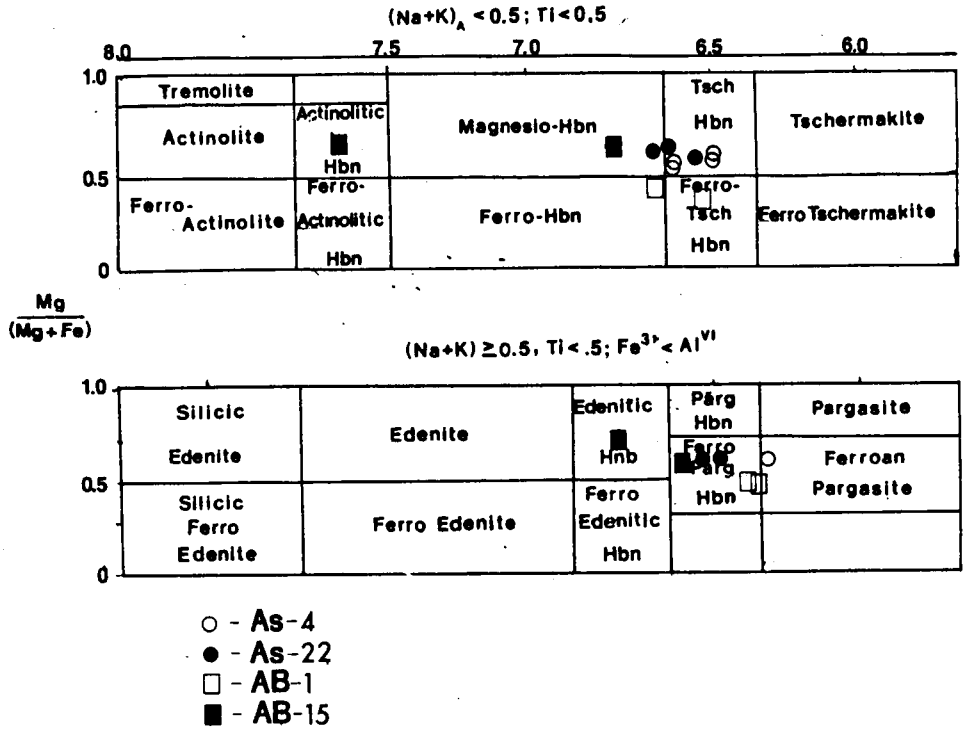

Figure 5. Nomenclature of amphiboles from this study (after Leake, 1978). (○) denotes As-4; (●) denotes As-22; (□) denotes AB-1; (■) denotes AB-15.

effect of increasing grade on samples from this study. Laird and Albee (1981) attributed the increase in A-site occupancy and Al^{VI} content with increasing metamorphic grade to increasing tschermakite and glaucophane substitution.

Plagioclase was analyzed in all samples and representative analyses are given in appendix D. Anorthite contents range between An_{18} and An_{35}. A plot of X_{An} vs. X_{Na} in amphibole (Figure 7) shows that samples from this study compare to similar plots from the garnet-oligoclase zone in other studies (e.g. Cooper, 1972).

Garnet grains were analyzed from 3 samples and representative analyses are given in appendix D. Compositions of garnets are all rich in the almandine component (X_{alm} = .75) with the pyrope and grossular components being subordinate and approximately equal. Individual grains show no appreciable compostional zoning and the range of compositions shown for As-22 represents the maximum compositional variation.

Compositions of ilmenite are given in appendix D. Microprobe analyses confirm the petrographic observation that only a small hematite component is present. Limited substitution for Fe has occurred in both samples. As-4 shows a small amount of geikelite ($MgTiO_3$) component,

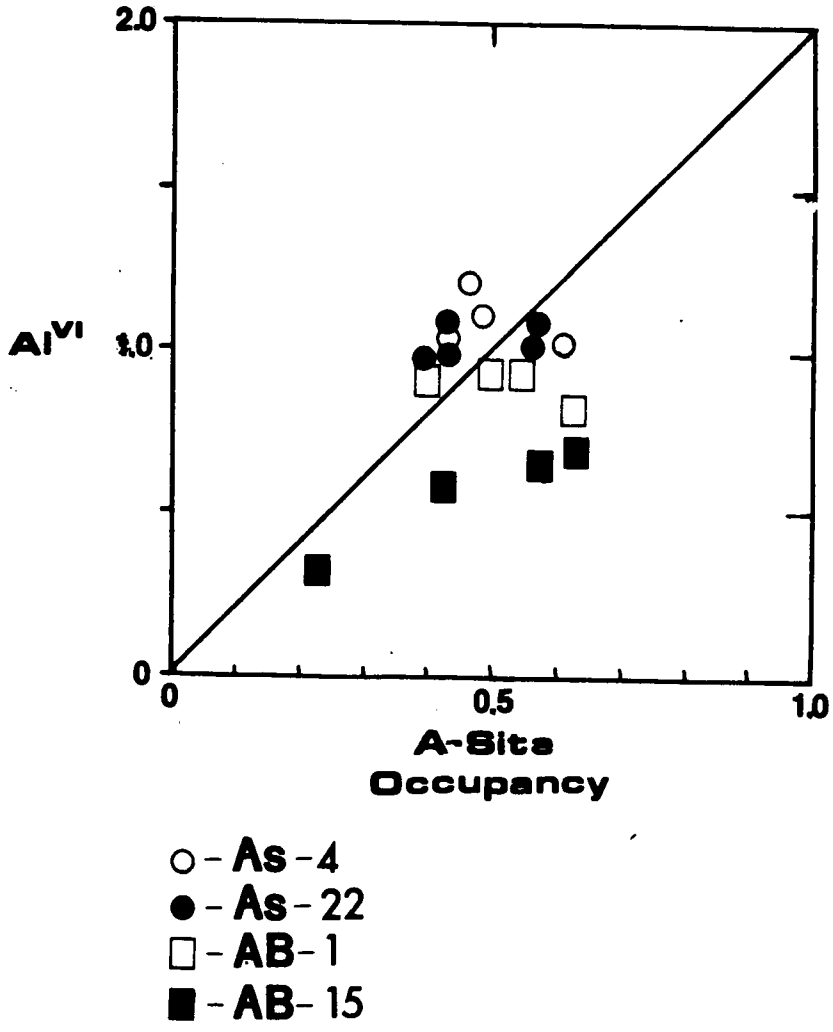

Figure 6. Al^{vi} versus A-site occupancy for selected hornblende analyses. Symbols are the same as those in figure 5.

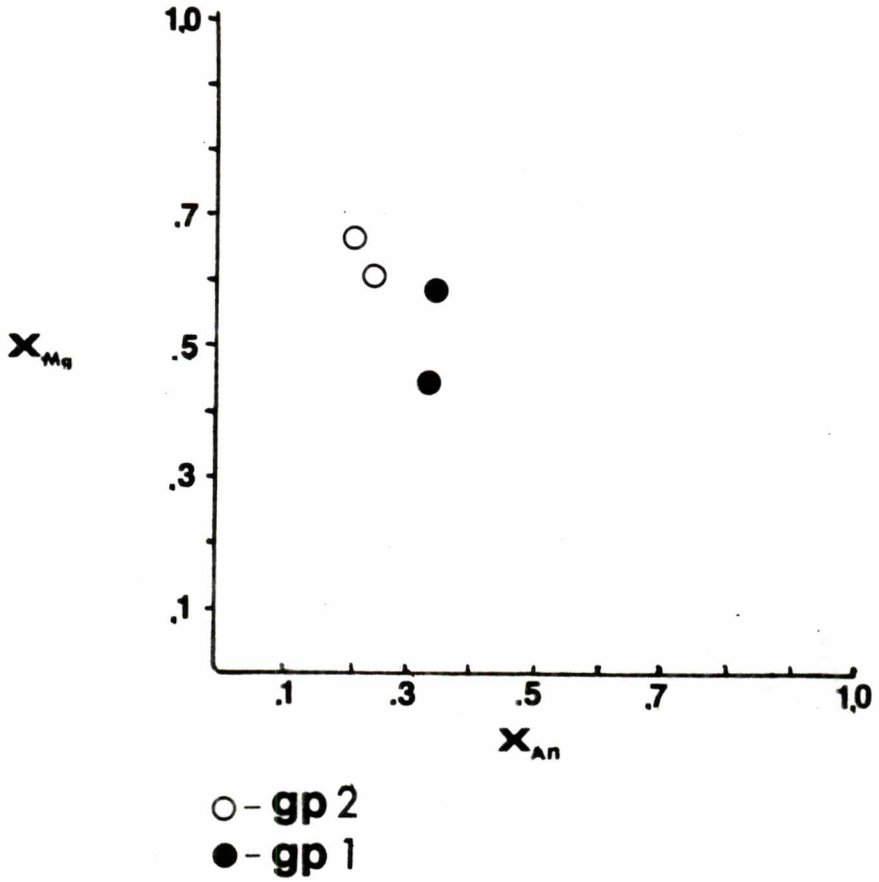

Figure 7. X_{Mg} in hornblende versus X_{An} in plagioclase of selected samples.

whereas ilmenite in As-22 shows substitution of pyrophanite ($MnTiO_3$).

Cummingtonite analyses from As-22 show that grains from this study have low percentages of trivalent cations, a trend typical for this mineral coexisting with hornblende (Robinson, 1982). Mg/Fe ratios for this sample are approximately 4.5:2.5.

Typical biotite (AB-1) and epidote (AB-15) analyses are also shown in appendix D. Because biotite was not examined in the Ashe Formation, it is difficult to assess the relation of Al^{IV} content and metamorphic grade. Epidote is characterized by low contents of Fe and Na. The association of epidote with a particular phase, either sulfide or oxide, has been found to be of some value in indicating relative metamorphic grade (Laird an Albee, 1981). The association of epidote in this sample with ilmenite coincides with this combination in other metamorphic terrains, and indicates a higher grade acheieved than for the coexistence of ilmenite and a sulfide.

CHAPTER 3

GEOCHEMISTRY

Introduction

As textural relationships, both on thin section and hand sample scales, and field relationships are often ambiguous, geochemical data are essential for interpreting the protolith of the amphibolites. Such an approach has been used successfully in earlier studies of southern Appalachian amphibolites (e.g. Achiabar, 1983; Stow et al., 1984).

It is important to recognize that some elements may be mobilized after rock emplacement, either by submarine weathering before regional metamorphism (e.g. Thompson, 1978) or during regional metamorphism (e.g. Rock et al., 1985; Stephenson, 1980; Floyd and Winchester, 1983). These studies show that major elements most susceptible to alteration are K and Fe^{3+} and to a lesser extent Ca and Mg. Minor and trace elements with large ionic radii such as Ba and Rb may also be mobilized by metamorphic processes. Rare earth elements, which are commonly used in studies of this type, are generally thought to be immobile; however, many workers (e.g. Nystrom, 1984) have suggested that rare earth elements may be mobilized during spillitization, especially in basalts relatively rich in

amygdules. The question of element mobility within samples from this study will be addressed in the following chapter.

Despite the fact that certain elements may be mobilized at various times during the rocks' history, use of discrimination diagrams based on ratios of trace elements that are considered immobile (Ti, V, Zr, Y, Nb, Cr, Ni, REE, Hf, Th, Ta) have been used extensively to determine tectonic affinities of basalts (e.g., Floyd and Winchester, 1975; Pearce and Cann, 1973; Shervais, 1982). Other elements that are probably slightly more mobile (Ca, Al, Fe, Mg) have been used to discriminate among different types of basalts (e.g., Pearce et al., 1977; Pearce and Cann, 1975); however such diagrams are not included in the present discussion because they utilize elements (such as K, Na) which are easily mobilized during metamorphism.

For this study 74 samples were chemically analyzed for their major and selected trace elements. Representative analyses are given in Table 1 and a complete listing of the analyses is given in Appendix B. In the discrimination diagrams discussed below no distinction has been made between the Ashe and Alligator Back samples as they do not show any apparent or statistical difference in mineralogic or chemical composition.

Table 2.1. Whole rock analyses of selected amphibolite samples from the Ashe and Alligator Back Formations (oxides in wt%; elements in ppm).

	Group 1		Group 2		Group 3
	As-12	AB-8	As-73	AB-9	As-71
Na2O	2.92	2.04	2.55	2.40	1.63
MgO	6.13	5.01	8.35	8.94	9.91
Al2O3	12.88	13.81	14.61	14.09	11.81
SiO2	47.89	50.24	49.72	49.84	47.46
P2O5	0.44	0.39	0.10	0.21	.00
K2O	0.27	0.92	1.23	0.26	0.30
CaO	9.79	8.17	10.82	10.89	12.67
MnO	0.21	0.21	0.15	0.14	0.20
FeO*	16.44	16.56	10.32	11.35	14.92
TiO2	3.23	3.13	0.94	1.34	0.39
V	315.00	249.00	288.00	252.00	392.00
Cr	330.00	224.00	216.00	300.00	636.00
Ni	93.00	68.00	67.00	97.00	161.00
Rb	2.00	12.00	38.60	4.00	7.00
Sr	140.00	276.00	175.00	163.00	44.00
Y	39.00	36.00	24.00	28.00	11.00
Zr	187.00	198.00	70.00	118.00	24.00
Nb	13.60	16.10	n.d.	10.00	n.d.
Total	100.31	100.96	98.86	99.57	99.43
Y/Nb	2.87	2.24	23.70	2.81	107.00
Zr/Y	4.79	5.50	2.95	4.20	2.24
Zr/Nb	13.75	12.30	70.00	11.80	240.00
Nb/Y	0.35	0.45	0.04	0.36	0.01
Mg#	39.83	34.94	58.95	58.30	54.11
Ti/V	106.00	61.47	56.97	42.91	70.42
Norms					
Q	---	3.33	----	----	----
or	1.66	5.44	7.39	1.60	1.83
ab	25.27	19.48	20.92	20.07	15.58
an	20.86	23.54	25.41	26.70	22.74
ne	---	----	----	----	----
	wo 10.6	6.17	12.16	10.91	16.81
di	en 4.7	2.45	7.25	6.35	9.26
	fs 5.9	3.83	4.34	4.09	7.01
	en 4.1	9.74	2.27	11.34	0.65
hy	fs 5.1	15.05	1.34	7.23	0.49
	fo 4.6	----	8.49	3.27	11.34
ol	fa 6.3	----	5.54	2.29	9.35
mt	4.80	4.75	2.92	3.19	4.11
ilm	5.14	5.13	1.84	2.51	0.84
ap	0.88	0.78	0.14	0.45	----

Protolith

Amphibolites may be derived from several different rock types and it is therefore necessary to determine whether the protolith is of sedimentary or igneous affinity (Leake, 1964). Leake (1964) suggested that a ternary plot of the Niggli values mg, c and al-alk provides a method for discriminating para- and ortho-amphibolites. A plot of these values for Ashe and Alligator Back amphibolites (figure 8) suggests that these rocks follow an igneous trend designated by the bold line.

The suggestion that the protoliths of the Ashe and Alligator Back amphibolites are igneous rocks is further substantiated by plots of [(Al + Fe + Ti)/3]-K vs. [(Al + Fe + Ti)/3]-Na (figure 9) and Al + Fe + Ti vs. Ca + Mg (figure 10) (Bard and Moine, 1979). In these plots almost all samples plot within the field of basalts, away from protoliths of sedimentary affinity. Also, only one sample (As-7) plots near the spillite field in figure 9, suggesting minimal sea floor alteration. From the discrimination diagrams discussed above, it is concluded that the protoliths for the Ashe and Alligator Back amphibolites were definitely igneous and most likely basalts. This supports the suggestions of previous workers based on field and regional relations (Rankin, 1970; Abbott and Raymond, 1984).

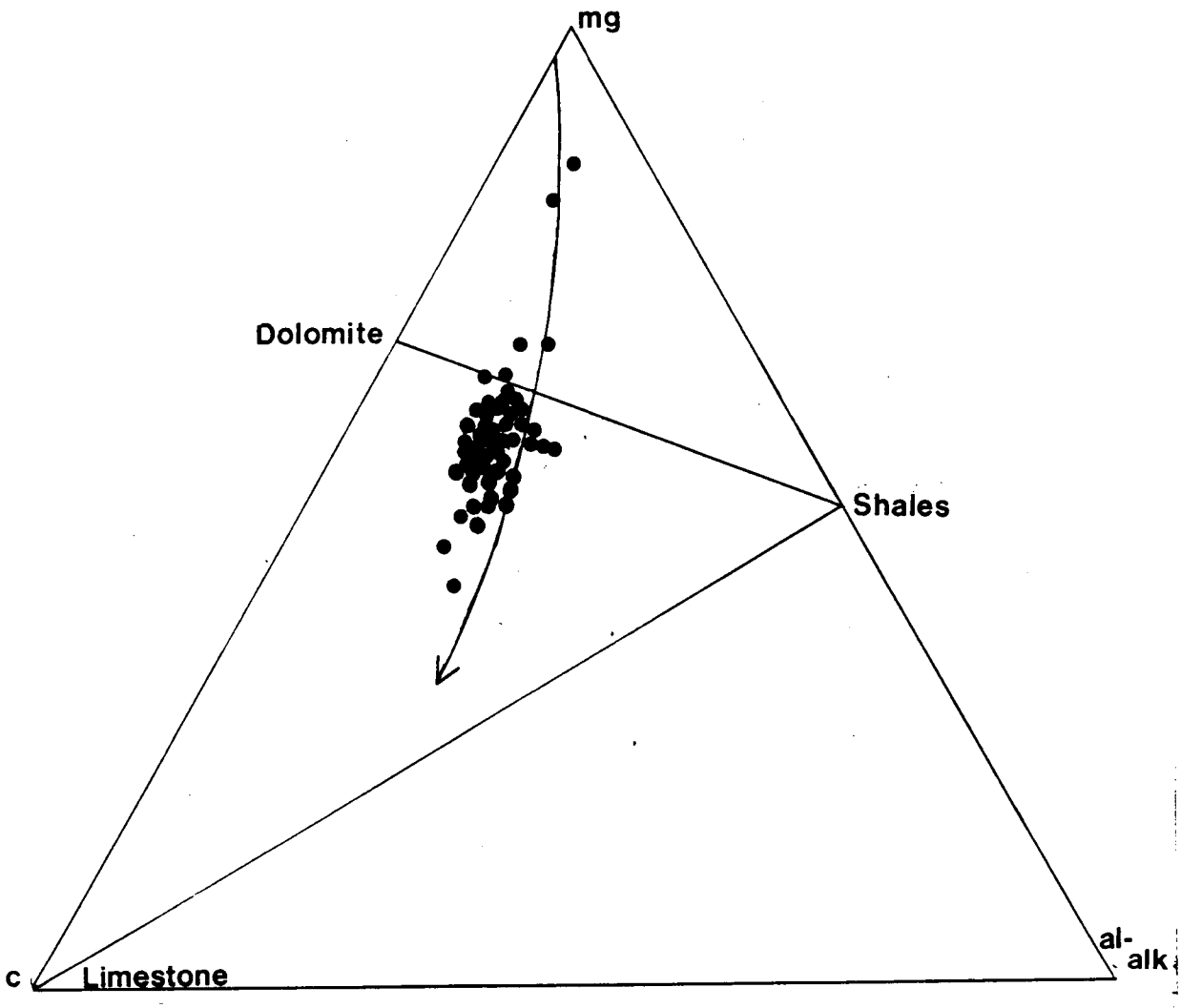

Figure 8. Niggli 100*mg - c - (al-alk) plot for amphibolites from the Ashe and Alligator Back Formations; mg = (MgO/FeO + MnO + MgO), c = CaO, al = Al_2O_3).

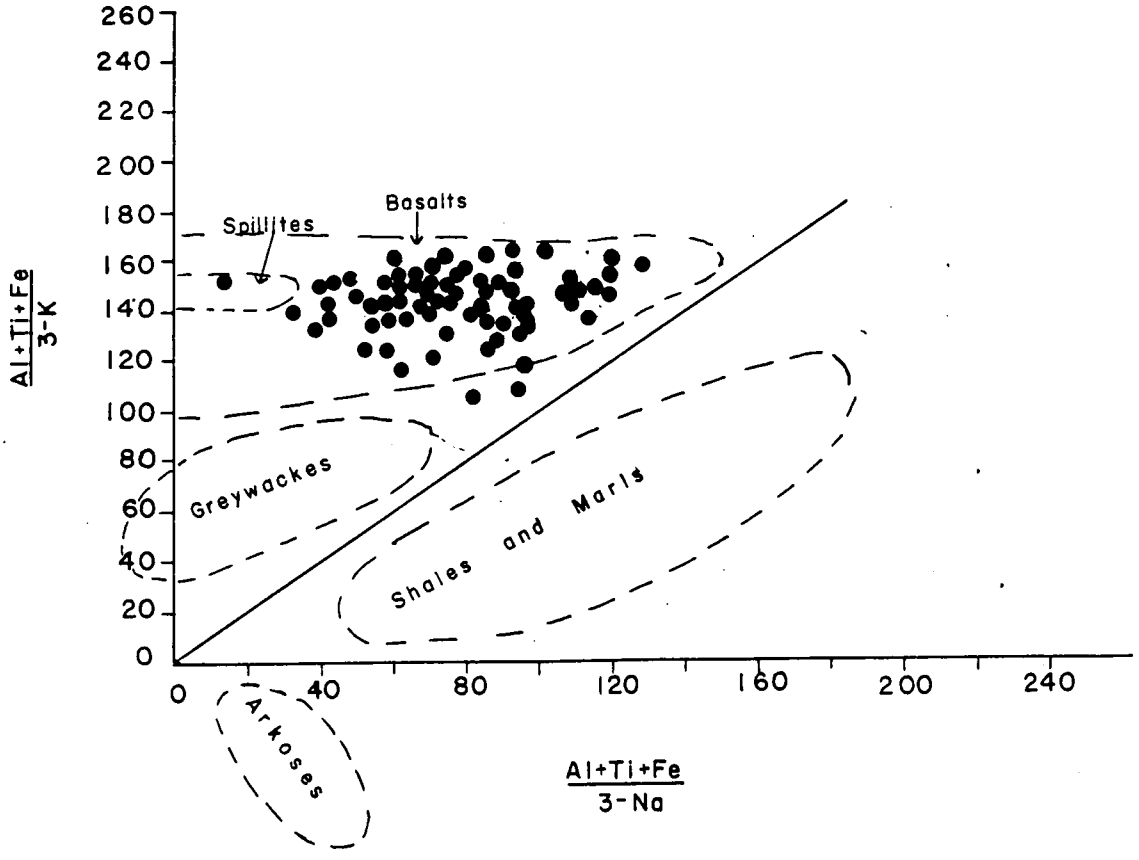

Figure 9. [(Al + Fe + Ti)/3] - K versus [(Al + Fe + Ti)/3] - Na discriminant diagram (after Bard and Moine, 1979) for amphibolites from the Ashe and Alligator Back Formations. Al, Fe, . . . etc., are the contents in millimoles of each element in 100 grams of rock.

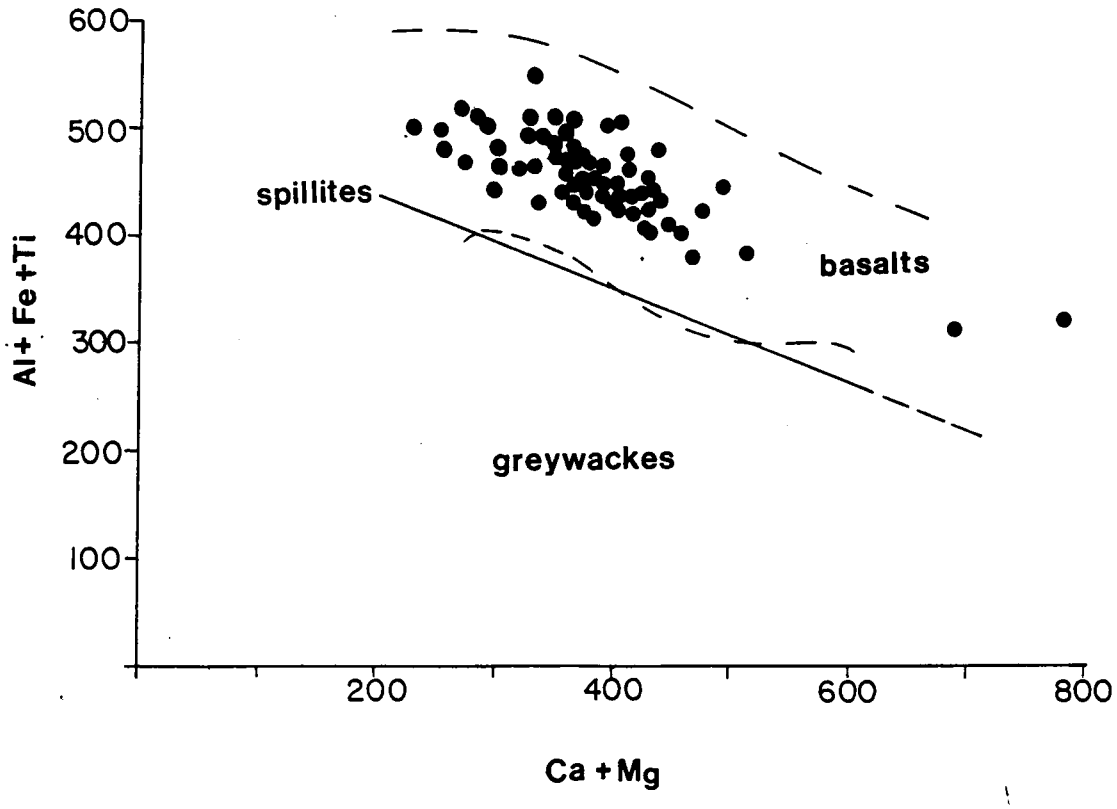

Figure 10. Al + Fe + Ti versus Ca + Mg discriminant diagram (after Bard and Moine, 1979) for amphibolites from the Ashe and Alligator Back Formations. Al, Fe, . . . etc., are the contents in millimoles of each element in 100 grams of rock.

The nature of the protolith can be refined further by using other discrimination plots. An A-F-M plot (figure 11) after Irvine and Baragar (1971) shows that the samples plot within the field of tholeiitic basalts. This conclusion, however, should be taken with some caution because the A-F-M plot is partially based on the alkali ($Na_2O + K_2O$) content of the sample. The concentrations of these elements are somewhat questionable because the elements (especially Na) are easily mobilized during metasomatism. It should be noted that two samples (As-10 and As-94) plot well outside the range of the other samples. Based on their extremely high MgO and low SiO_2 values, these samples appear to represent metamorphosed ultramafic rocks and, therefore, will be excluded from further discussion.

Figure 12, a plot of Nb/Y vs. Zr/P_2O_5*100 (Floyd and Winchester, 1975), also shows that almost all samples plot as tholeiites, with only four samples plotting close to the boundary for alkalic basalts. This figure supports the conclusion drawn from the A-F-M plot that samples from this study are tholeiitic basalts.

Variation diagrams cconstitute an integral part of any study of igneous rocks as they may provide clues about crystallization of a magma, as well as about metasomatism and/or alteration of the rocks. In choosing a fractionation index (abscissa) for these samples many

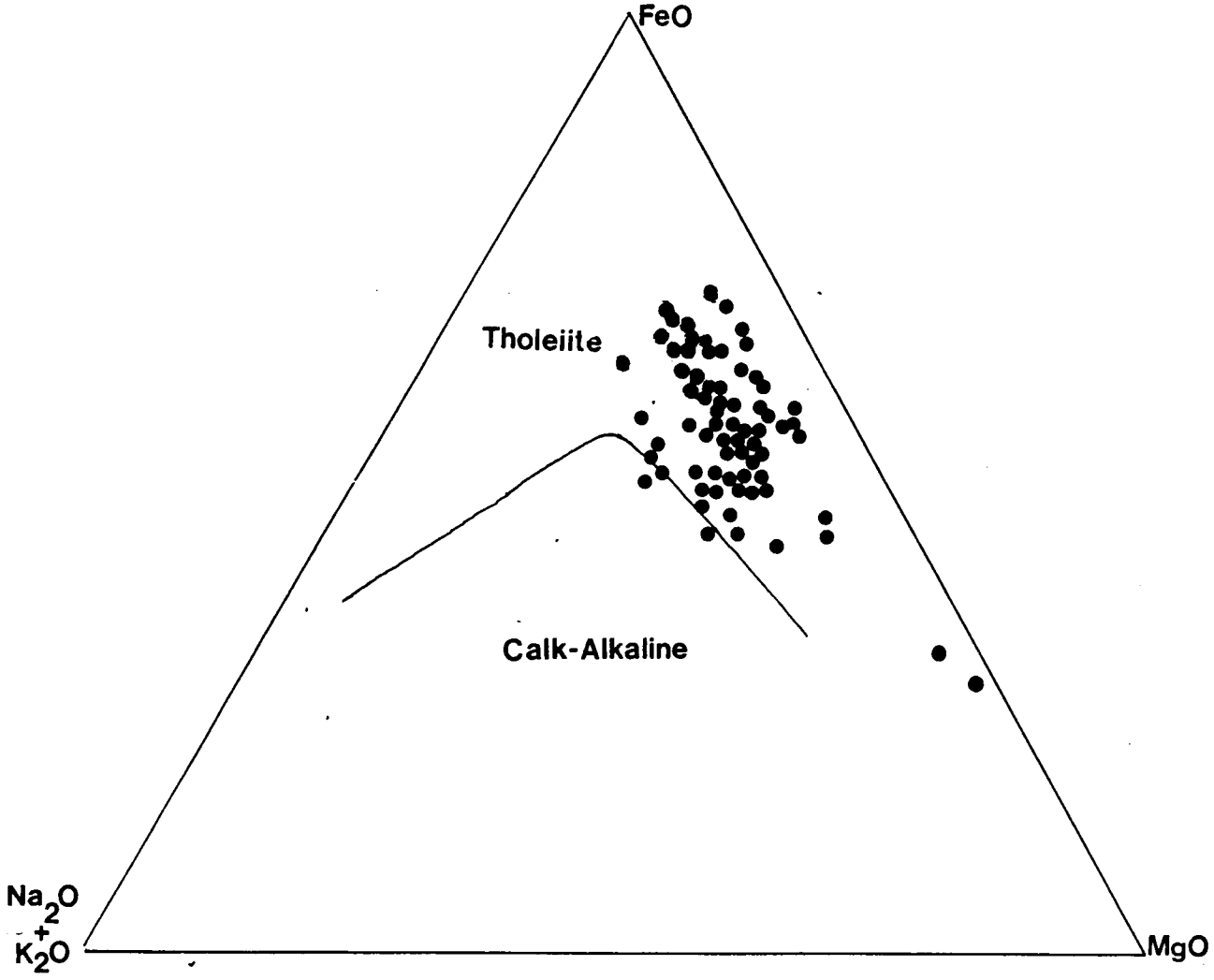

Figure 11. AFM plot of amphibolites from the Ashe and Alligator Back Formations. Tholeiitic--calc-alkaline boundary after Irvine and Barager (1971).

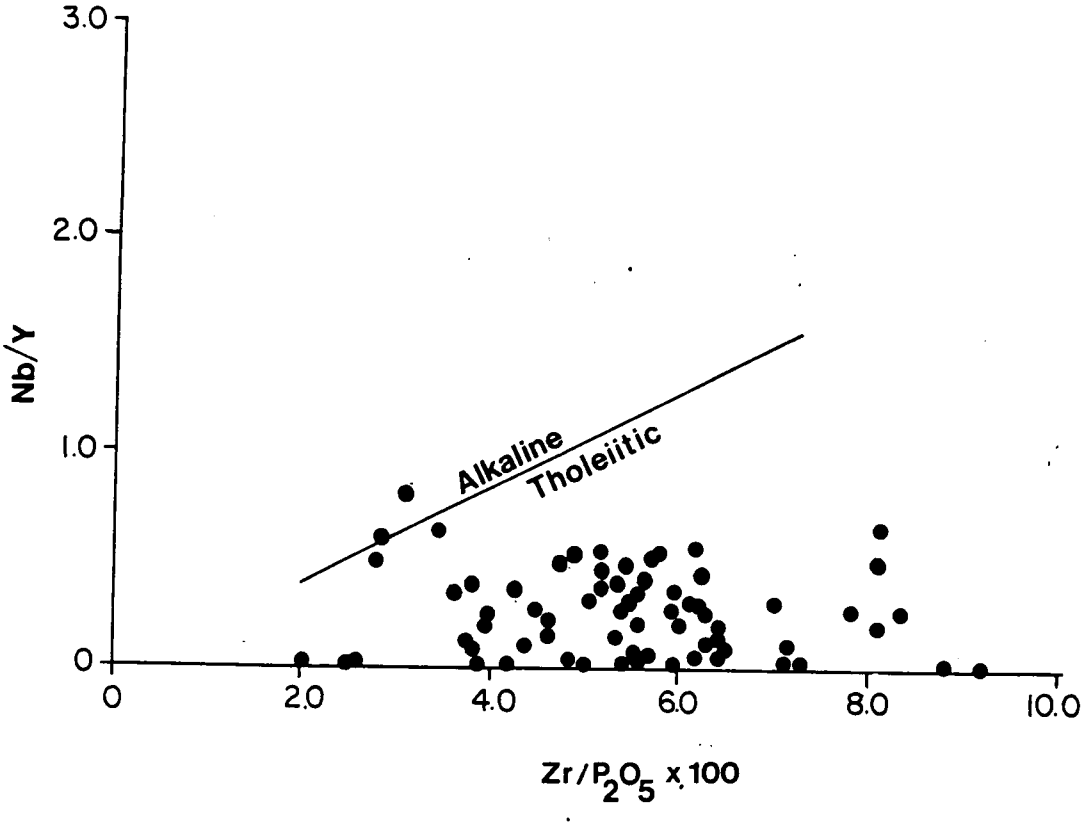

Figure 12. Nb/Y versus $(Zr/P_2O_5)*100$ discrimination diagram (after Floyd and Winchester, 1975) for amphibolites from the Ashe and Alligator Back Formations.

elements or groups of elements were tested (MgO, Mg number, MgO/FeO*, mafic index); however, trends for many plots were scattered. The use of Zr as a fractionation index eliminates much scatter, and yields reasonable trends (figure 13).

Several trends are apparent from inspection of variation diagrams. Rocks from this study show enrichment in the incompatible elements Ti, Nb, Sr, Y and P with progressive differentiation. Conversely, the elements Ca, Mg and Ni are depleted with progressive enbrichment in Zr. Al_2O_3 and Fe_2O_3* values appear to be antithetic; however, this relationship may be fortuitous. Trends for V show an increase then decrease with differentiation. The decrease in V probably indicates the onset of the fractionation of magnetite and will be important in evaluation of the Ti/V discriminant diagram. The scatter in the diagrams for Na_2O, SiO_2, K_2O and Rb suggests that these elements have probably undergone some degree of metasomatism.

Two observations from these diagrams have important implications for the following sections of this report. First, many elements retain ostensibly igneous trends, suggesting that these elements were not significantly affected by post-depositional processes. Second, the trends of the immobile elements suggest that fractionation is responsible for the wide range im compositions. This

Figure 13. Variation diagrams of selected major element oxides (weight %) and trace elements (ppm) plotted against Zr

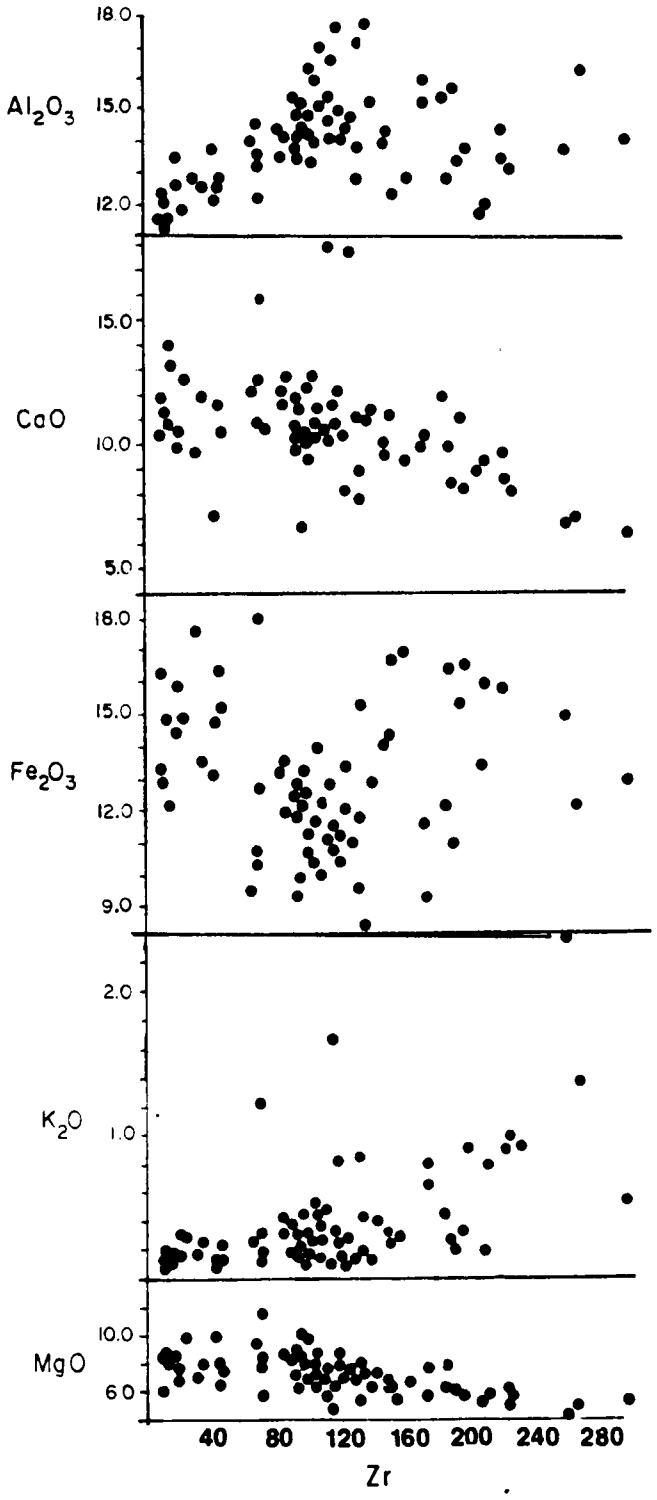
Al_2O_3
18.0
15.0
12.0
CaO
15.0
10.0
5.0
Fe_2O_3
18.0
15.0
12.0
9.0
K_2O
2.0
1.0
MgO
10.0
6.0
40
80
120
160
200
240
280
Zr

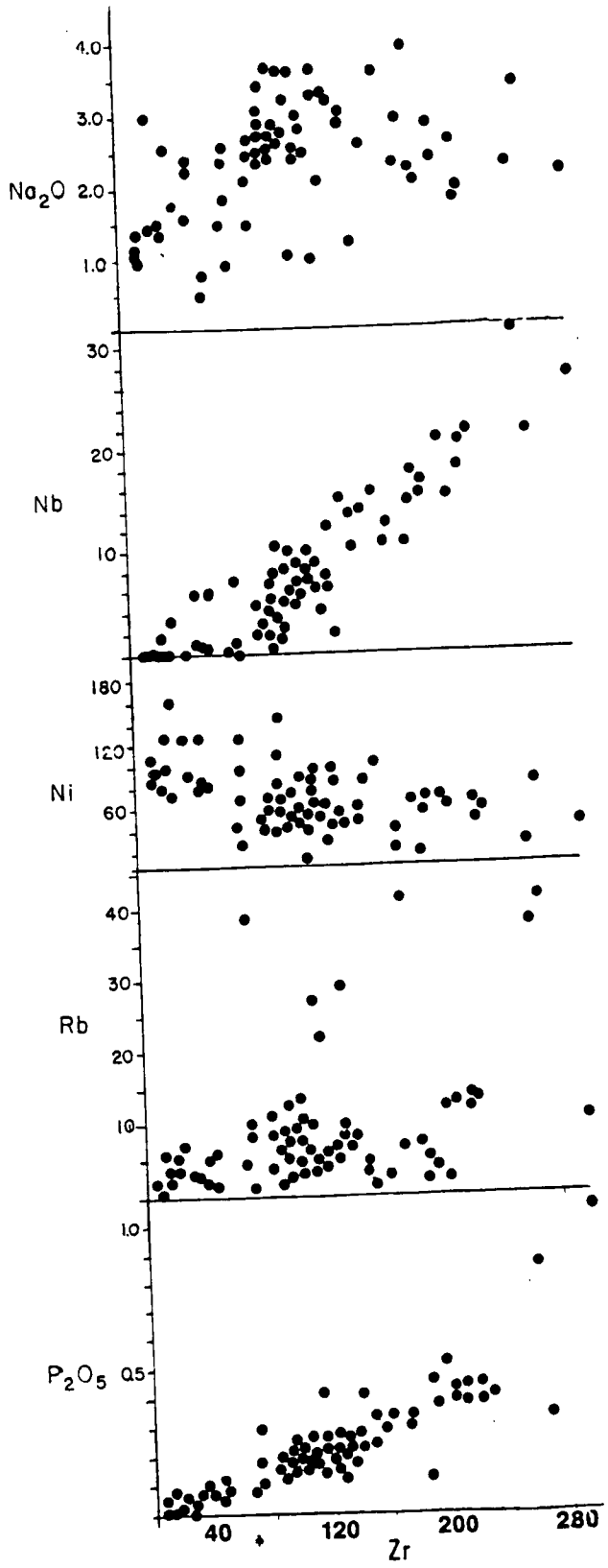
4.0
3.0
Na_2O 2.0
1.0
30
20
Nb
10
180
120
Ni
60
40
30
Rb
20
10
1.0
P_2O_5 0.5
40
120
200
280
Zr

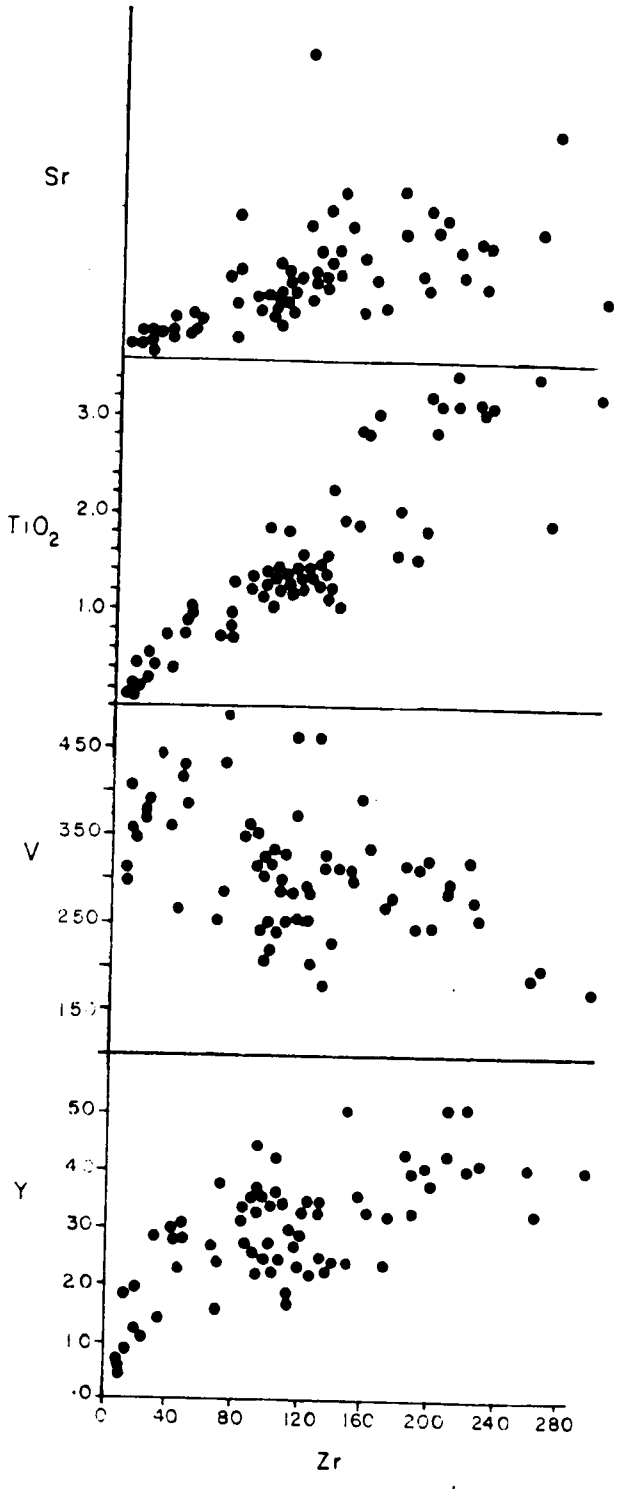
Sr
TiO2
3.0
2.0
1.0
V
450
350
250
Y
50
40
30
20
10
0
0
40
80
120
160
200
240
280
Zr

hypothesis will be considered in more detail in the following sections.

Tectonic Setting

Several plots of immobile elements have been published in the literature to distinguish basalts of various tectonic settings. In this section these will be used to assess the teconic setting of mafic rocks from the Ashe and Alligator Back Formations.

Several discriminant diagrams have been used to distinguish ocean floor basalts from subduction-related and continental basalts. A plot of Ti/100 - Zr - Y*3 (figure 14) after Pearce and Cann (1973), shows that samples from this study are concentrated in the within-plate and ocean floor basalt fields (designated herein as group 1 and group 2, respectively). The group of samples plotted as open circles (group 3) show no consistent affinity for any tectonic field, but they apparently follow a trend established by the samples in the ocean floor field. Four samples, AB-1, As-68, As-74 and As-5, plot in the field of calc-alkaline basalts, but three of them plot quite close to field boundaries. Based on their consistent positions in the discriminant diagrams discussed later, AB-1 has been assigned the same symbol as within-plate basalts and As-68 and As-74 the same symbol as ocean floor basalts. As-5, however, is anomalous and

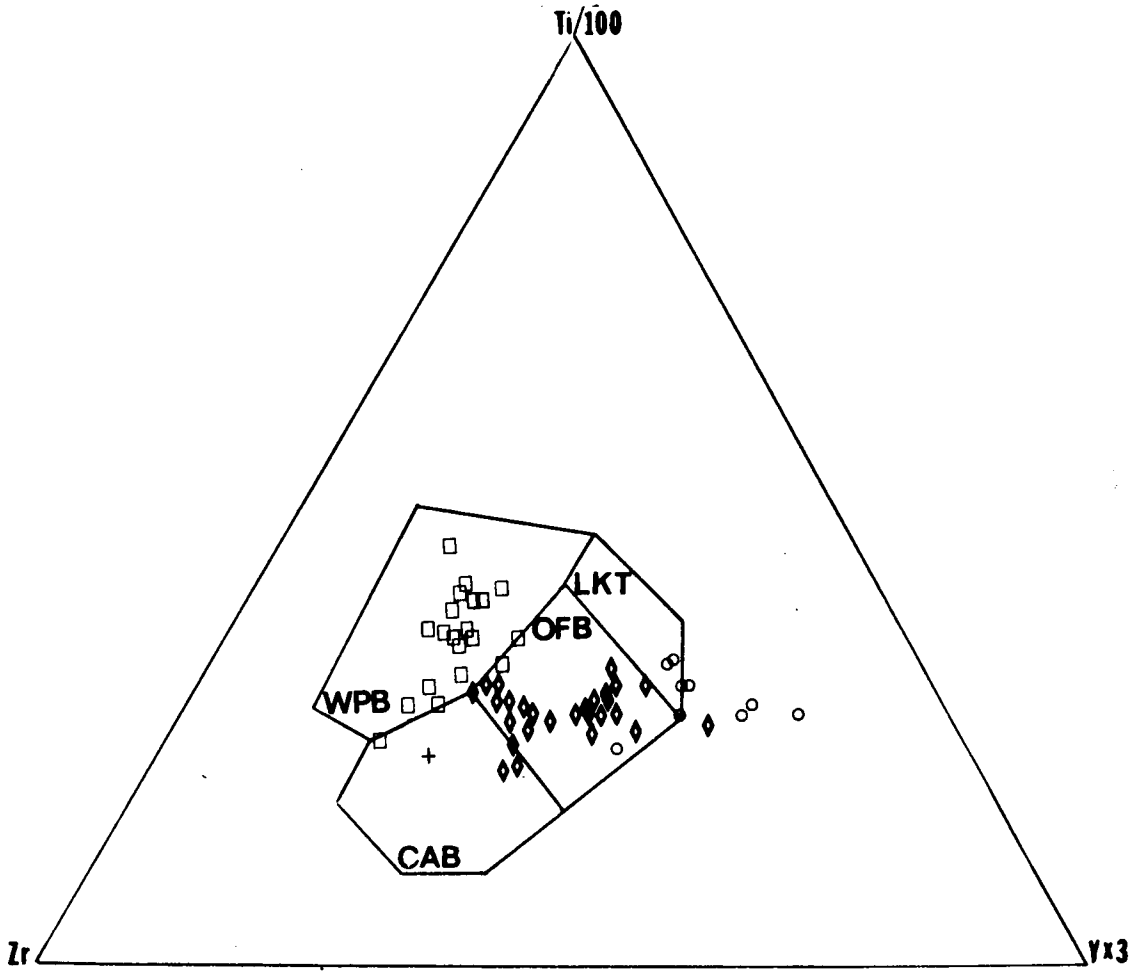

Figure 14. Ti/100 - Zr - Y*3 discrimination diagram (after Pearce and Cann, 1973) for amphibolites from the Ashe and Alligator Back Formations. (□) denotes group1; (◊) denotes group 2 and (○) denotes group 3. WPB = Within Plate Basalts; LKT = Low Potassium Tholeiites; OFB = Ocean Floor Basalts; CAB = Calc-Alkaline Basalts.

will be eliminated from further analyses. Several (15) samples do not meet the screen (12% < CaO + MgO < 20%) established for this diagram. These samples are not plotted on this diagram and their ommission does not effect the chemical grouping. On the following discriminant diagrams these samples will be used because the plots do not employ the above mentioned chemical screen.

Logarithmic plots of TiO_2 vs. Zr and Zr/Y vs. Zr have also been used as effective discriminant diagrams (Pearce and Norry, 1979). When amphibolites of the Ashe and Alligator Back Formations are plotted on these diagrams (figure 15), groups similar to those on the Ti/100-Zr-Y*3 diagram can be rcognized: Group 1 rocks show within plate characteristics, whereas group 2 samples plot mainly in the ocean floor basalt field. Significantly, some samples from group 2 overlap into the within-plate field on the Zr/Y-Zr plot, but they do not overlap into the area dominated by within-plate basalts. Samples from group 3 are scattered and cannot be assigned to any particular tectonic setting.

Shervais (1982) summarized the theory describing the behavior of Ti and V in igneous processes and then combined the theory with published analyses of basalts to arrive at a discrimination diagram based on these two elements (figure 16). This figure, like the other

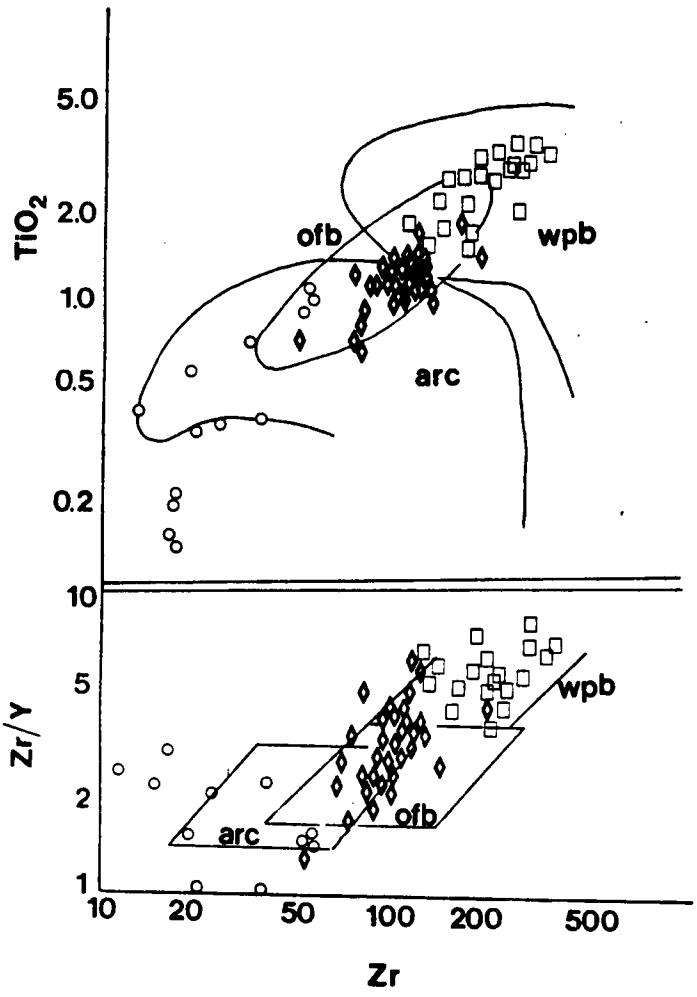

Figure 15. Logarithmic TiO_2 versus Zr and Zr/Y versus Zr discrimination diagrams (after Pearce and Norry, 1979) for amphibolites from the Ashe and Aligator Back Formations. WPB = Within Plate Basalts; OFB = Ocean Floor Basalts; ARC = Low Potassium tholeiites + Calc-alkaline basalts. Symbols are the same as those used in figure 14.

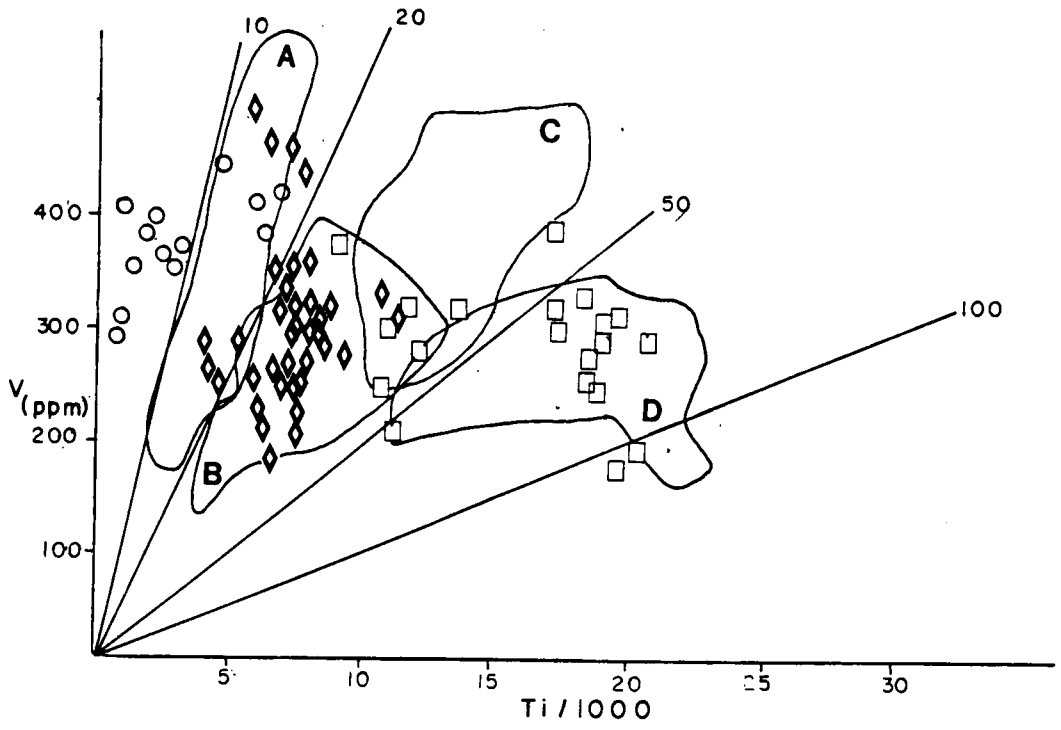

Figure 16. V versus Ti/1000 discrimination diagram (after Shervais, 1982) for amphibolites from the Ashe and Alligator Back Formations. Symbols are the same as those used in figure 14. A = Subduction related basalts; B = Mid-ocean Ridge Basalts; C = Continental Flood Basalts; D = Ocean Island and Alkalic basalts.

discriminant plots, shows good delineation of two of the groups with group 1 rocks plotting in the alkali basalt field and group 2 samples clustered in or near the MORB field. The Ti/V ratios of group 3 are clearly anomalously low for basalts.

The Ti/V diagram is also an effective discriminant between continental flood basalts and oceanic island basalts. According to Shervais (1982) continental flood basalts have Ti/V ratios similar to MORB (20-50), whereas oceanic island basalts have Ti/V ratios closer to 100; overlap between the two groups is minimal. On this basis it appears that the Ti/V ratios of group 1 rocks reflect basalts formed in an oceanic island; however, inspection of the data (figure 13, variation diagrams) reveals that, for group 1 samples V decreases with progressive differentiation. This process is indicative of fractionation of magnetite, and may lead to anomalously high Ti/V ratios. If this process occurs the Ti/V discriminant diagram for those rocks may not be useful (Shervais, 1982).

Figure 17 (after Floyd and Winchester, 1975) yields further discrimination, placing group 1 samples in the continental tholeiite field and group 2 basalts in the oceanic tholeiite field. Many samples have a Y/Nb ratio of > 13 and do not plot on this figure. These include 9 samples from group 2 and 11 from group 3. This diagram is

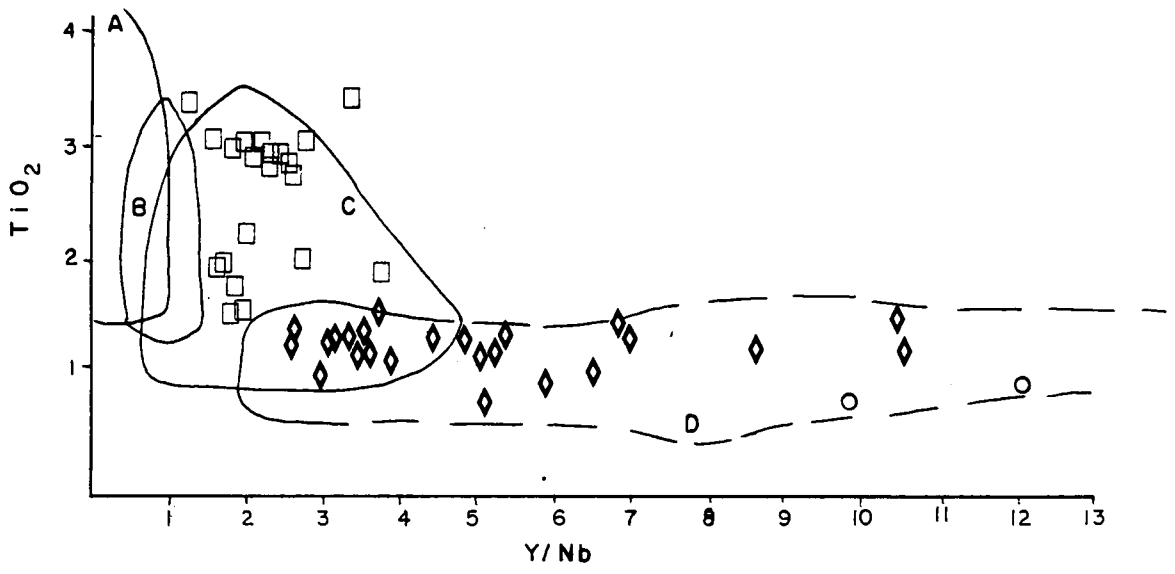

Figure 17. TiO_2 versus Y/Nb discrimination diagram (after Floyd and Winchester, 1975) for amphibolites from the Ashe and Alligator Back Formations. Symbols are the same as those used in figure 14. A = oceanic alkalic basalts; B = continental alkali basalts; C = continental tholeiites; D = oceanic tholeiites.

important in that is supports previously discussed discrimination plots and it also indicates that group 1 samples are of continental, not oceanic island affinity.

Within the past few years much new chemical data have been obtained on processes active at mid-ocean ridges. These studies have illustrated that several types of basalt may exist at or near these structures. These included N-type (normal, depleted), T-type (transitional) and P-type (plume, enriched) basalts. The P-type basalts usually occur off-axis and are thought to be a product of an N-type source being contaminated by an enriched P-type source (LeRoex et al., 1981). The source of the enriched material is thought to be associated with a mantle plume or 'hot spot'. The following discussion will explore the similarities or differences between group 1 and 2 rocks from this study and samples gathered from present-day ocean basins.

A ternary plot of Zr/Nb - Zr/Y - Y/Nb (after Fodor and Vetter, 1984) is shown in figure 18. This diagram demonstrates that samples inferred to represent within-plate basalts on the basis of other discrimination diagrams, plot away from the P-type field but close to lavas of continental flood basalt affinity. This supports the hypothesis that group 1 rocks are of continental rather than ocean island character. Other

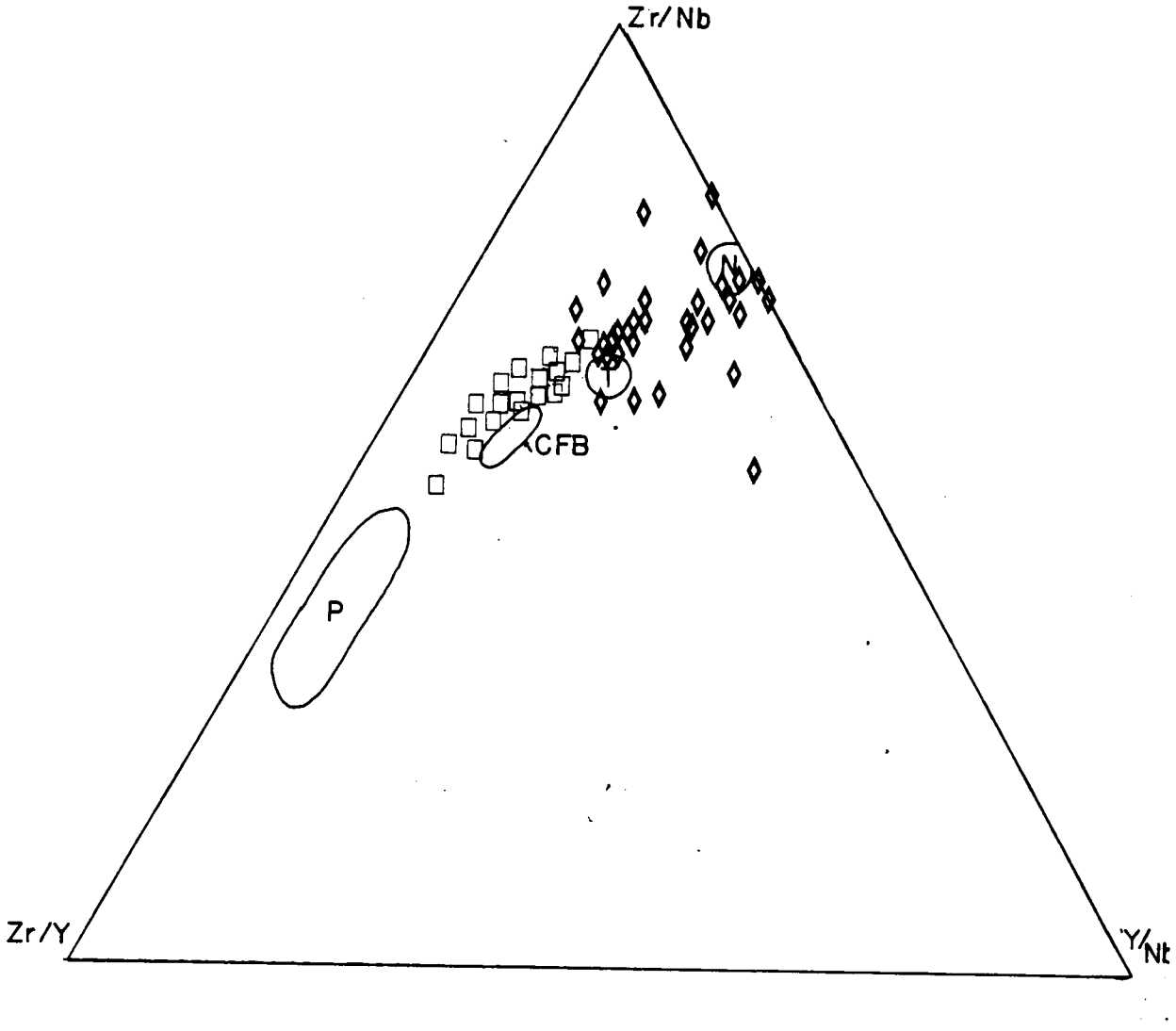

Figure 18. Zr/Nb - Y/Nb - Zr/Y discrimination diagram (after Fodor and Vetter, 1984) for amphibolites from the Ashe and Alligator Back Formations. Symbols are the same as those used in figure 14. N - N-type (depleted) basalt; T - T-type (transitional) basalt; P - P-type (Plume) basalt ; N, T and P-type basalt fields after LeRoex et al. (1983). CFB = Continental Flood Basalts from Espirito Santo Basin, Brazil (after Fodor and Vetter, 1985).

samples plot close to the Zr/Nb - Y/Nb axis, thus indicating their correlation with N-type basalts.

Finally, a plot of TiO_2 vs. FeO*/MgO (figure 19) appears to clarify some of the ambiguity presented by the previous discrimination diagrams. Group 1 samples have a continental character, whereas remaining group 2 samples plot as T-type basalts. Thus this diagram strongly supports the postulates derived from the previous diagram that group 1 rocks are of continental affinity, whereas group 2 rocks are ocean floor tholeiites. This diagram also suggests that ocean floor tholeiites are closely related to T-type (transitional) basalts, but some are N-type (depleted).

Rare earth element data are presented in figure 20 and patterns from these samples support conclusions derived from discrimination diagrams. Two samples from group 1, As-12 and As-96, yield nearly identical patterns showing enrichment in LREE and abundances of 20-40X chondrites. This type of pattern is characteristic of continental basalts from many areas including the Deccan traps (Alexander, 1977), South American Mesozoic basins (Fodor and Vetter, 1984), and North Americal Mesozoic basins (Gottfried et al., 1983). Group 3 rocks are unusual in that they show slight enrichment of LREE and strong enrichment of HREE. The low abundances of REE in samples from group 3 are suggestive of intrusive rocks.

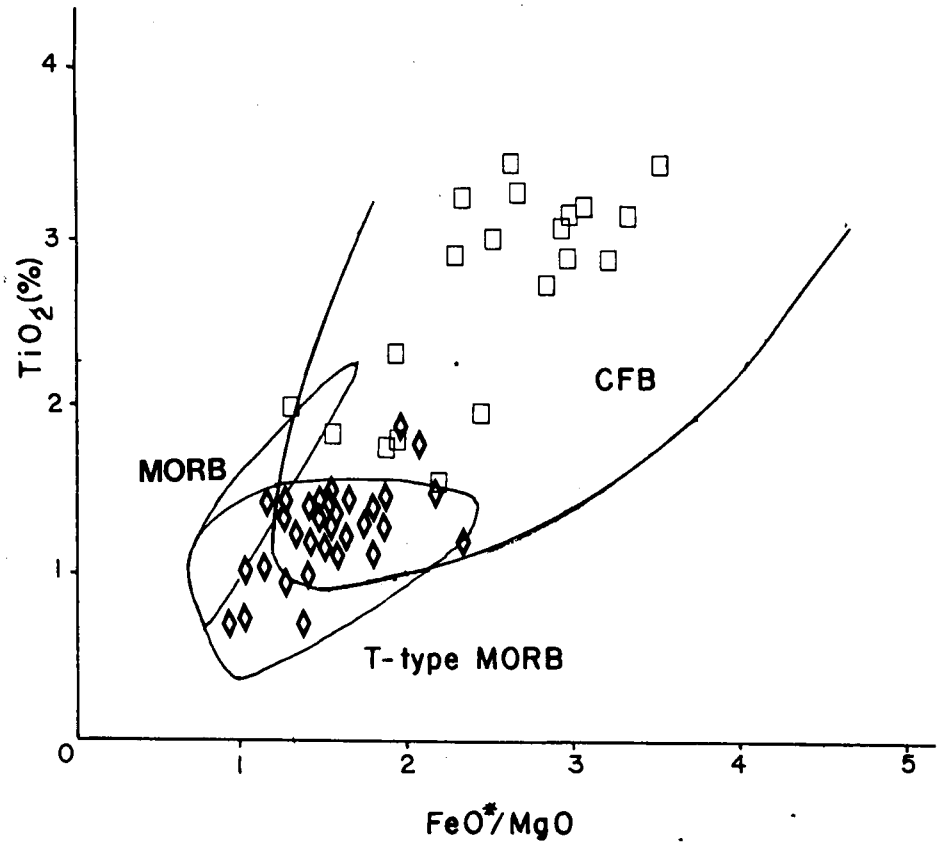

Figure 19. TiO_2 versus FeO*/MgO discrimination diagram (after Fodor and Vetter, 1984) for amphibolites from the Ashe and Alligator Back Formations. Symbols are the same as those used in figure 14. CFB = Continental Flood Basalts; MORB = Mid-ocean Ridge Basalts; T-type MORB = Transitional Mid-ocean ridge basalt.

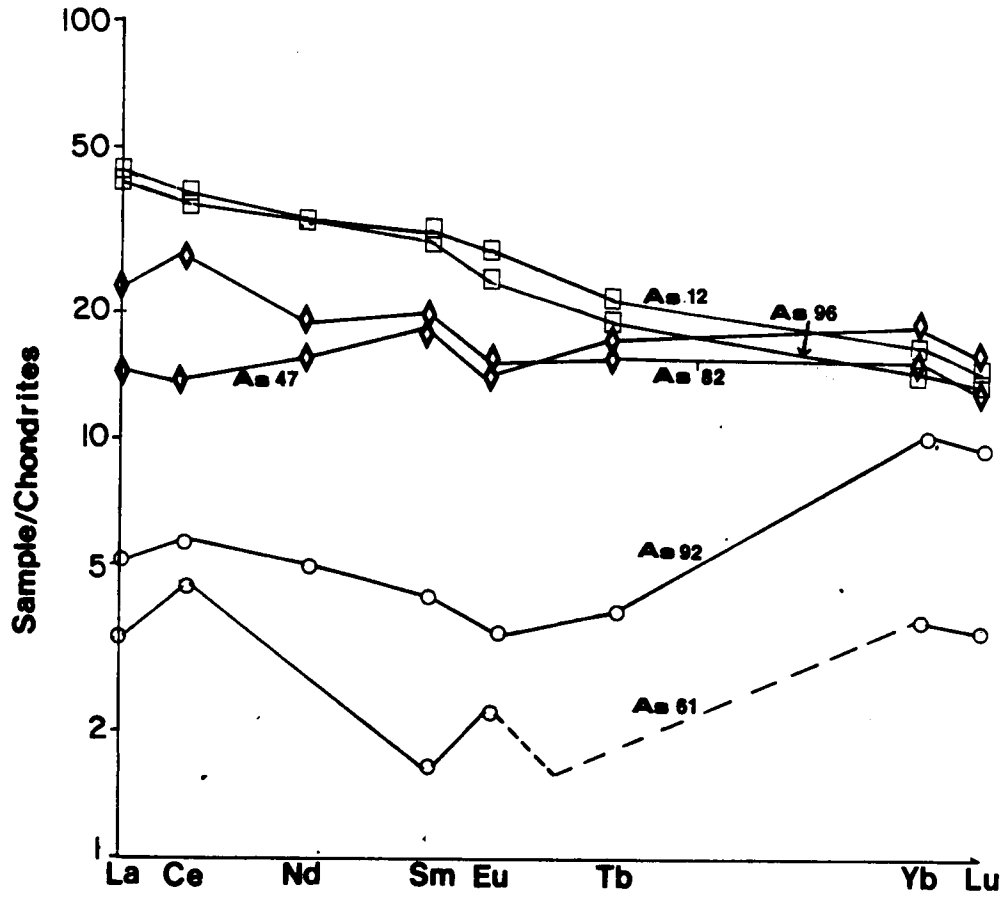

Figure 20. Chondrite-nornalized REE patterns from selected amphibolites from the Ashe Formation. Normalization values are from Thompson et al. (1982).

Group 2 samples are relatively flat with values of 10-20X chondrites and are typical of MORB (Basaltic Volcanism Study project, 1981). Samples As-47 and As-82 also show small negative Eu anomalies that may suggest these samples were derived from plagioclase-enriched intrusive rocks illustrated by As-61. More detailed modeling is necessary to evaluate this possibility.

It is interesting to note the spatial relationship of the samples inferred to represent different tectonic settings (Figure 21). Samples from groups 1 and 2 occur throughout both formations, whereas those from group 3 are found only in the Ashe. There also seems to be a pattern in the spatial distribution of the basalt types: group 2 basalts occur dominantly in the southwest, whereas groups 1 and 3 are concentrated in the northeastern part of the study area.

In summary, several trends are apparent from the discrimination diagrams (Table 2): (1) On diagrams that delineate plate tectonic setting, group 1 samples all consistently fall in or near a witin-plate setting. On the basis of discriminant diagrams such as figure 17 (p.52)(Floyd and Winchester, 1975) and figure 18 (p.54)(Fodor and Vetter, 1984), it appears that these are of continental flood basalt affinity rather than oceanic island or P-type basalt; (2) group 2 rocks fall into two plate tectonic settings: most samples from group 2 plot as

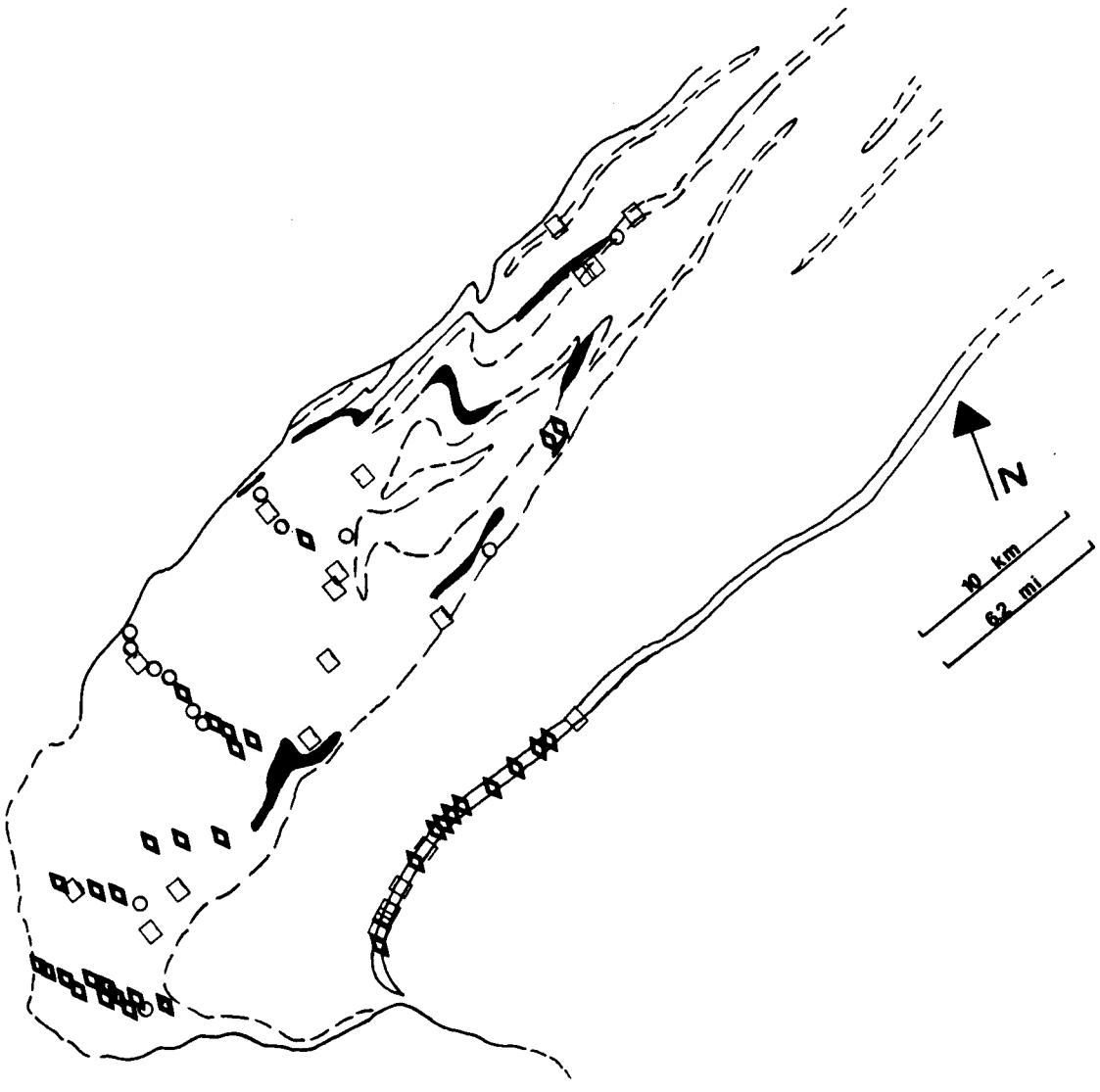

Figure 21. Map showing location of samples with respect to geochemistry. Symbols are the same as those used in figure 14.

Table 3.2 Summary of inferred protoliths for amphibolites of the Ashe and Alligator Back Formations.

Chemical Group	Protolith	Distribution
1	within-plate basalt	As + A. B.
2	intrusive rock (?)	Ashe
3	ocean floor basalt	As + A.B.

ocean floor basalts and fall into fields of T and N-type mid-ocean ridge basalts, but on the Zr/Y-Zr diagram some samples overlap into the within-plate field; and (3) group 3 rocks, which occur only in the Ashe Formation, show no consistent correlation to any plate tectonic setting based on trace element analysis. This fact, coupled with their high Ca, Mg and Ni contents leads to the conclusion that these may represent intrusive rocks or phenocryst-enriched basalts.

CHAPTER 4

DISCUSSION

Element Mobility

The data presented in the preceding section have important implications on previous interpretations for the tectonic setting of the Ashe Formation. Because the samples have been metamorphosed, however, it is important to include some discussion on element mobility. This process and its magnitude have been attributed to several causes. These include low-grade hydrothermal alteration and metamorphism and high grade regional metamorphism. Element mobility in the latter group may be enhanced by interaction with various types of country rocks (Rock et al., 1985), the presence of meta-shear zones (Floyd and Winchester, 1983) and high CO_2 levels in the fluid phase during metamorphism (Hynes, 1980). Rare earth elements, especially La, although possibly not mobilized by high grade metamorphism, have been shown to be mobilized during hydrothermal alteration, especially in vesicular lavas (Hellman and Henderson, 1977; Nystrom, 1984). Humphris et al. (1978) have also suggested that REE mobility may be a product of the igneous crystallization history of the sample or suite.

At this point it is not possible to quantify element mobility, but the qualitative relevance of several factors will be discussed here. Hydrothermal alteration has been shown to have the greatest effects on the elements Fe, K, Na, Rb and Sr. Variation diagrams of these elements (Figure 13, p. 42) plotted against Zr show some scatter, especially within K_2O, Na_2O and Rb trends. Sr and Fe_2O_3*, despite showing some scatter, reveal relatively coherent trends. It cannot be unequivocally concluded that scatter of K_2O, Na_2O and Rb is caused by hydrothermal alteration, but it is a possibility. Immobile elements (Ti, V, Y, etc.) show little or no scatter in these trends, thus indicating that sea floor alteration of these elements in samples from this study was minimal.

Interaction with country rocks has been described as another process in which movement of mobile and immobile elements may occur. Rock et al. (1985) suggested that the character of the host rock (e.g. limestone, pelite, sandstone, granite gneiss) influences the particular element that is mobilized, thus influencing the metamorphic mineral assemblage. Although interaction between country rocks and amphibolites probably occurs, it is likely to be important only in small podiform and thinly layered amphibolites. In the study area of the Ashe Formation, amphibolite clearly is the dominant rock

type and samples were rarely collected from an area proximal to an observed contact with non-amphibolitic rock. Therefore, it is considered that country rock-amphibolite interaction was not an influential process in the post-depositional history of this suite of rocks.

The formation of meta-shear zones is another geological process which is thought to cause element mobility, especially for the elements K, Rb and Ba (Floyd and Winchester, 1983). It was also suggested that Ca, Mg, Sr, Na and Mn are enriched by these processes. Although this area of the Ashe Formation has been mapped on a scale of 1:250,000 in most areas and on a scale of 1:62,500 in the Jefferson, Warrensville and Zionville Quadrangles, no major shear zones have been described. There is a random relationship between sample locations and chemical groups, thereby negating a relationship between structure and chemistry. This fact, along with the lack of observed shear zones, argues against the possibility of structural features disturbing the original chemical composition of the protolith.

Another possible mechanism for altering original whole-rock geochemistry is the presence of metamorphic fluids high in CO_2 (Hynes, 1980). Hynes used several lines of reasoning to arrive at this conclusion for metavolcanic rocks of the Ascot Formation, Quebec. These

included (1) a wide range of immobile element concentrations for a small range in major element composition; (2) unusually low contents of TiO_2 and Zr (.25 wt.% and 5 ppm, respectively); (3) no correlation between TiO_2 and Zr content and the extent of differentiation, and (4) samples plotting over a broad field on Pearce and Cann's (1973) Ti-Zr-Y diagram.

The samples of Ashe and Alligator Back Formations studied show a wide range of trace element concentrations, including what appear to be anomalously low contents of TiO_2, Zr and other immobile elements. This is the primary characteristic of group 3 rocks. Although these are anomalously low for basalts, they are characteristic of intrusive mafic rocks. Original igneous textures have been obliterated due to the high degree of metamorphism. It is, therefore, possible that this wide range of values is original. This is supported by the fact that variation trends (Figure 13, p. 42) consistently show these samples to be less evolved than their ostensibly extrusive counterparts. This observation is in contrast to data from the unit described by Hynes (1980).

Finally, samples from this study, like samples from the Ascot Formation, plot over a broad field on Pearce and Cann's Ti-Zr-Y diagram. Although it is possible that this may reflect element mobility, the fields defined for groups 1 and 2 rocks on the Ti-Zr-Y diagram are

consistently corroborated by other discriminant plots. Further, the fields defined for these samples correspond to tectonic settings which appear to be reasonable for the known stratigraphic and structural framework of the area. Group 3 rocks show variability on all discriminant diagrams, but this aberration, like the group's low trace element contents, is most likely caused by the original composition of the rock. As will be discussed below, the presence of intrusive rocks in the Ashe should not be considered surprising. Finally, the composition of metamorphic fluids that were present in the Ashe has not been determined; however, from field work it is known that little carbonate rock is present within this area of the formation and that calcite is a rare constituent of these samples. Based on the above discussion, it is concluded that analyses similar to those found in the Ascot Formation may be attributed to protolith composition and not post-depositional element mobility.

Another factor which must be considered when evaluating the geochemistry of metamorphosed basalts is the effect of metamorphic segregation. Evidence of this process is manifested in amphibolites of the Ashe by thick (up to 20 cm) bands of plagioclase and quartz. Because these bands are not representative of the amphibolites, areas with concentrations of such layers were avoided during sampling. On a smaller scale distinct mineralogies

should be expected for the observed geochemical groups if element mobility during regional metamorphism is the cause of these trends. In this study such a relationship between chemistry and mineralogy is not observed. Hornblende and plagioclase concentrations are quite variable throughout the study samples and minerals not present in all samples (garnet, biotite, ilmenite and sphene) show no preference for any chemical group. Finally, the presence of well-defined igneous differentiation trends for all trace elements and most major elements in this study indicates that chemical characteristics inherent in the protoliths were able to survive the rigors of regional metamorphism without significant alteration.

Validity of Discriminant Diagram

A problem inherent in any study using discriminant diagrams in which within-plate basalts are suggested is the applicability of the Ti-Zr-Y diagram to continental tholeiites. This question has been raised by Holm (1982) who showed that some known continental tholeiites did not plot on the within-plate basalt field of the Ti-Zr-Y diagram. Although this may be true, the fact that samples from the within-plate field consistently plot in the same field on other diagrams suggests that the Ti-Zr-Y plot is accurate for samples from this study.

A more fundamental problem with these diagrams is the effectiveness of discriminant plots in dealing with highly fractionated basalts. If, as is suggested by variation diagrams (Figure 13, p. 42), all samples are related by one fractionation, then the suggestion that the Ashe Formation was deposited in two distinct plate tectonic settings may be specious. However, in a study of mid-ocean ridge basalts from the Conrad Fracture Zone, LeRoex and Dick (1981) calculated that basalts whose incompatible elements (Ti, P, Y, Nb) plotted in a linear fashion against Zr could have evolved from two parental magmas. Moreover, when these highly fractionated samples (up to 3.5% TiO_2) are placed on Pearce and Cann's Ti-Zr-Y diagram, they show a trend from the mid-ocean ridge field into the calc-alkaline field, not the within-plate field.

Regional Setting

The geochemistry of the amphibolites, on the basis of empirical discriminant diagrams show a close association of within-plate basalts and ocean floor basalts. The occurrence of these two types of basalts is consistent with previous suggestions that the Ashe Formation was deposited during initial rifting and formation of a "proto-Atlantic" Ocean. The results are also consistent with the data presented by Gair and Slack (1984) for the Ashe Formation in southwestern Virginia.

The possible identification of group 3 rocks as an intrusive phase is interesting because many workers describe the Ashe as being metamorphosed tholeiitic basalts. On the basis of "relict gabbroic textures" Rankin (1970) suggested that some shallow intrusive rocks were present in the Ashe; however, samples from this study reveal no relationship between texture and chemistry; i.e. both coarse and fine-grained amphibolites are present in all chemical groups.

Data for these rocks are ambiguous in the sense that trace, including rare earth, element abundances suggest a protolith of plutonic rock, whereas major element (Mg/Mg + Fe) concentrations are not high enough to be considered characteristic of such rocks. Also, the CaO + MgO totals for some of these samples, as well as some samples from group 2, are sometimes greater than 20%, a general dividing line between intrusive and extrusive rocks. Discrimination diagram analysis reveals no consistent tectonic setting for these samples. Diagrams such as the Ti/100-Zr-Y*3 plot suggest an association with ocean floor basalts, whereas others (Figure 16, p. 50) imply formation in a volcanic arc or subduction zone. The latter setting is improbable because regional field evidence and other geochemical data from this study indicate the presence of an extensional tectonic regime. Rare earth element patterns of group 3 samples from this

study are similar to those seen in alpine-type dunites and harzburgites (Frey, 1984), but differ in that the rare earth element abundances are higher. It is possible that these samples may not represent ultramafic rocks, but may have been originally basalts with abundant phenocrysts of olivine or olivine and orthopyroxene. Because no original phenocrysts are present, it is difficult to corroborate this suggestion. It is likely therefore that the protolith for rocks from group 3 contained a high solid/liquid ratio. Whether the rocks are of cumulate or extrusive origin is difficult to determine.

The delineation of distinct chemical groups of basalts and amphibolites (groups 1 and 2 in this study) is also consistent with observations from rocks assumed to be of similar age in the northern Appalachians (Coish et al., 1985), as well as suites of rocks from other known continental and oceanic settings. episodes. The latter includes the Precambrian Keeweenewan rift (Wilband and Wasunavlich, 1980), the early Mesozoic North Atlantic margin (Weigland and Ragland, 1970), the early-mid Mesozoic Brazilian margin (Fodor and Vetter, 1984; Montovani et al., 1985) and the lower Tertiary plateau basalts of east Greenland (Larsen and Watt, 1985).

It should be noted that the extent to which rifting proceeded in this study area is questionable because of deformational events that followed deposition of the Ashe.

Although basalts from the areas stated above possess geochemical signatures similar to those of the Ashe, rifting in these locations advanced to different stages, from failure of a purely continental rift (Keweenawan) to the formation of a large ocean (Mesozoic Atlantic margins). Thus, although the bulk of the data indicates the presence of an extensional tectonic regime, care must be taken not to constrain the tectonic environment beyond the limitations of the geochemical data.

The chemical data from this study thus provide some guidelines for evaluating the depositional site for the Ashe. Briefly, the suggested models are: (1) deposition on a passive, ensialic margin; (2) deposition on a passive, ensimatic or transitional margin with a sedimentary source of the North American craton to the west; (3) deposition on an active, ensimatic margin where the source of sediments was the Piedmont Island Arc to the east; and (4) formation in a back arc basin.

The first three models are all similar in that they invoke deposition between the North American continent and the island arc which possibly existed near the present-day Carolina Slate Belt to the east. The models differ in that model (1) requires deposition associated with the North American continent, model (2) suggests deposition on transitional or a combination of ensimatic and ensialic crust, and model (3) suggests formation at a mid-ocean

ridge and later obduction onto and sedimentation from the island arc.

From data presented here, it appears that model (1) is inaccurate because characteristics of both oceanic and continental crust are apparently represented, with oceanic crust being the more dominant type. Model (3), although it contains facets of both types of crusts, incorporates subduction beneath the Piedmont island arc to the east. No subduction-related volcanism was determined from this study, thus this aspect of model (3) is questionable.

Based on the nature of ultramafic bodies in the Ashe and the lack of remnants of a volcanic arc, Abbott and Raymond (1984) suggested that model (4) was not applicable to the Ashe. Data from this study show little evidence of volcanic arc activity, thus supporting their hypothesis; however, delineation of back arc basin and ocean floor basalts is difficult because they possess similar geochemical signatures. This observation, coupled with the fact that the study area has been intensely deformed makes it unlikely that the separation of ocean floor and back-arc basin tectonic settings can be further refined from a geochemical approach.

Conclusions from this study imply an area proximal to both ensialic and ensimatic crust as is proposed in model (2). Following deposition, during the Taconic Orogeny, the Ashe was probably dismembered and thrust

westward. Ultramafic rocks supposedly represent mantle rocks, whereas the amphibolite component is metamorphosed oceanic crust. This model may be further refined from this study by the identification of an intrusive phase. Thus, the presence of basalts, possible intrusive rocks, ultramafic rocks and a diverse sedimentary sequence, suggests that the Ashe has many of the trappings of a 'melange', as suggested by Abbott and Raymond (1984) and Raymond and Swanson (1981).

CHAPTER 5

CONCLUSIONS

The conclusions from this study are summarized below:

(1) Amphibolites from this area of the Ashe and Alligator Back Formations adhere to igneous trends, thus indicating their derivation from igneous protoliths.

(2) It is apparent from the geochemical data that three different groups of igneous rocks occur in the study area: Group 1 rocks contain high concentrations of incompatible elements and low values of Mg, Ca and Ni; samples from group 2 are manifested by a large range of trace element concentrations, encompassing the range of values between those defined by groups 1 and 3; group 3 rocks contain unusually low contents of incompatible elements and relatively high values of Mg, Ca and Ni.

(3) On the basis of several published discriminant diagrams that utilize incompatible elements, it is concluded that group 1 rocks are representative of continental flood basalts, group 2 samples have characteristics of ocean floor basalts and group 3 samples are metamorphosed intrusive rocks or phenocryst enriched basalts.

(4) Based on regional field relations and history and the occurrence of similar geochemical fingerprints, it is

suggested that rocks from the study area were formed on a continental margin undergoing rifting.

REFERENCES

REFERENCES

Abbott, R., and Raymond, L., 1984, The Ashe Metamorphic Suite, northwest North Carolina: metamorphism and observations on geologic history: Amer. Jour. Sci., v. 84, p. 350-375.

Abrams, C., and McConnell, K., 1984, Geologic setting of volcanogenic base and precious metal deposits of the west Georgia Piedmont: A multiply deformed metavolcanic terrain: Econ. Geol., v. 79, p. 1521-1539.

Achaibar, J., 1983, A petrologic and geochemical study of some amphibolite bodies in the Smith River Allochthon, Virginia: M.S. thesis, University of Tennessee, 93p.

Albee, A.L., and Ray, L., 1970, Correction factors for electron probe microanalyses of silicates, oxides, carbonates, phosphates and sulphates: Anal. Chem., v. 42, p. 1408-1414.

Alexander, P.O., and Gibson, I.L., 1977, Rare earth abundances in Deccan Trap basalts: Lithos, v. 10, p.143-147.

Bard, J.P., and Moine, B., 1979, Acebuches amphibolites in the Aracena Hercynian metamorphic belt (SW Spain): geochemical variations and basaltic affinities: Lithos, v. 12 no. 4, p. 271-282.

Basaltic Volcanism Study Project, 1981, Basaltic volcanism on the terrestrial planets: New York, Pergammon Press, 1286 p.

Bence, A.E., and Albee, A.L., 1968, Empirical correction factors for the electron microanalysis of silicates and oxides: Jour. Geol., v. 76, p. 382-403.

Bryant, B., and Reed, J.C., Jr., 1970, Geology of the Grandfather Mountain Window and Vicinity, North Carolina and Tennessee: U.S. Geol. Survey Prof. Paper 615, 195p.

Coish, R.A., Fleming, S.A., Larsen, M., Poyner, R., and Seibert, J., 1985, Early rift history of the proto-Atlantic ocean: Geochemical evidence from metavolcanic rocks in Vermont: Amer. Jour. Sci., v. 285, p. 351-378.

Cook, F.A., and Oliver, J.E., 1981, The late Precambrian-early Paleozoic continental edge in the Appalachian orogen: American Journal of Science, v. 281, p. 993-1008.

Cooper, A.F., 1972, Progressive metamorphism of metabasite rocks from the Haast Schist group of southern New Zealand: Jour. Petrology, v. 13, p. 457-492.

Dupuy, C., and Dostal, J., 1984, Trace element geochemistry of some continental tholeiites: Earth and Planetary Sci. Lett.: v. 67, p. 61-69.

Floyd, P.A., and Winchester, J.A., 1975, Magma type and tectonic setting discrimination using immobile elements: EPSL, v. 27, no. 2, p. 211-215.

_____, 1983, Element mobility associated with meta-shear zones within the Ben Hope amphibolite suite, Scotland: Chem. Geol., v. 39, p. 1-15.

Fodor, R.V., and Vetter, S.K., 1984, Rift zone magmatism: Petrology of basaltic rocks transitional from CFB to MORB, southeastern Brazil margin: Contr. Min. Pet., v. 88, p. 307-321.

Frey, F.A., 1984, Rare earth element abundances in upper mantle rocks in Rare Earth Element Geochemistry, ed.,

Gair, J.E., and Slack, J.F., 1984, Deformation, geochemistry and origin of massive sulfide deposits, Gossan lead district, Virginia: Econ. Geol., v. 79, pp.1483-1520.

Gottfried, D., Annell, C.S., and Byerly, G.R., 1983, Geochemistry and tectonic significance of subsurface basalts near Charleston, South Carolina: Clubhouse Crossroads test holes #2 and #3: U.S. Geol Survey Prof. Paper 1313-A, p. A1-A19.

Hatcher, R.D., Jr., 1978, Tectonics of the western Piedmont and Blue Ridge, southern Appalachians: Review and Speculation: Amer. Jour. Sci., v. 278, p. 276-304.

Hellman, P.L., and Henderson, P., 1977, Are rare earth elements mobile during spilitisation?: Nature, v. 267, p. 38-40.

Holm, P.E., 1982, Nonrecognition of continental tholeiites using the Ti-Zr-Y diagram: Contr. Min. Pet., v. 79, p. 308-310.

Humphris, S.E., Morrison, M.A., and Thompson, R.N., 1978, Influence of rock crystallisation history upon subsequent lanthanide mobility during hydrothermal alteration in basalts: Chem. Geol., v. 23, p. 125-137.

Hynes, A., 1980, Carbonitization and mobility of Ti, Y and Zr in Ascot Formation metabasalts, SE Quebec: Contr. Min. Pet., v. 75, p. 79-87.

Irvine, T.N., and Bargar, W.R.A., 1971, A guide for the chemical classification of common volcanic rocks: Can Jour. Earth Sci, v. 8, p. 523-548.

Jones, T.A., 1976, Petrography, structure and metamorphic history of the Warrensville and Jefferson Quadrangles, southern Blue Ridge, northwestern North Carolina: Ph. D. thesis, Miami Univ. of Ohio, 130 p.

Laird, J, and Albee, A., 1981, Pressure, temperature, and time indicators in mafic schist: Their application to reconstructing the polymetamorphic history of Vermont: Amer. Jour. Sci., v. 281, p. 127-175.

Larsen, L.M., and Watt, W.S., 1985, Episodic volcanism during break-up of the North Atlantic: evidence from the east Greenland plateau basalts: Earth and Planet. Sci. Lett., v. 73, p. 105-116.

Leake, B.E., 1964, The chemical distinction between ortho- and para- amphibolites: Jour. Pet., v. 5, pt. 2, p. 238-254.

_____, 1978, Nomenclature of amphiboles: Amer. Mineralogist, v. 63, p. 1023-1053.

le Roex, A.P., and Dick, H.J.B., 1981, Petrography and geochemistry of basaltic rocks from the Conrad fracture zone on the America-Antarctica ridge: Eartn and Planet. Sci. Lett., v. 54, p. 117-138.

le Roex, A.P., Erlank, A.J., and Needham, H.J., 1981, Geochemical and mineralogical evidence for the occurrence of at least three distinct magma types in the "FAMOUS" region: Contr. Min. Pet., v. 77, p. 24-37.

McElhaney, M.S. and McSween, HJ.Y., 1983, Petrology of the Chunky Gal mafic-ultramafic complex, North Carolina: Geol. Soc. Amer. Bull., v. 94, p. 855-874.

Montovani, M.S.M., Marques, L.S., DeSousa, M.A. Civetta, L., Atalla, L., and Innocenti, F., 1985, Trace element and strontium isotope constraints on the origin and evolution of Parana continental flood basalts of Santa Catarina State (southern Brazil): Jour. Petrology, v. 26, p. 187-209.

Nystrom, J.O., 1984, Rare earth element mobility in vesicular lava during low-grade metamorphism: Contr. Min. Pet., v. 88, p. 328-331.

Odom, A.L., and Fullager, P.D., 1984, Rb-Sr whole rock and inherited zircon ages of the plutonic suite of the Crossnore complex, southern Appalachians, and their implications regarding the time of opening of the Iapetus Ocean: Geol. Soc. Amer. Spec. Paper 194, p. 255-261.

Pavlides, L., 1981, The central Virginia volcanic-plutonic island arc of Cambrian (?) age: U.S. Geol. Survey Prof. Paper 1231A, 44p.

Pearce, J.A., and Cann, J.P., 1973, Tectonic setting of basic volcanic rocks determined using trace element analyses: EPSL, v. 19, p. 290-300.

Pearce, J.A., Gorman, B.E., and Birkett, T.C., 1974, The TiO_2-K_2O-P_2O_5 diagram: a metod of discriminating between oceanic and nonoceanic basalts: EPSL, v. 24, p. 419-426.

Pearce, J.A., 1977, The relationship between major element chemistry and tectonic environment of basic and intermediate volcanic rocks: Earth Plan. Sci. Letters, v. 36, p. 121-132.

Pearce, J.A., and Norry, M.J., 1979, Petrogenetic implications of Ti, Zr, Y, and Nb variations in volcanic rocks: Contr. Min. Pet., v. 69, p. 33-47.

Rankin, D.W., 1970, Stratigraphy and structure of Precambrian rocks in northwestern North Carolina: in Fisher, G.W., Pettijohn, F.J., Reed, J.C., Jr., and Weaver, K.N., eds., Studies of Appalachian Geology: central and southern: New York, Intersci. Pub. (John Wiley), p. 227-245.

_____, 1975, The continental margin of eastern North America in the southern Appalachians: The opening of the proto-Atlantic Ocean: Amer. Jour. Sci., v. 275-A, p. 298-336.

Rankin, D.W., Espenshade, G.H., and Neumann, R.B., 1972, Geologic map of the west half of the Winston-Salem Quadrangle, North Carolina, Virginia, and Tennessee: U.S. Geol. Survey Misc. Invest. Map I-709-A, scale 1:250,000.

Rankin, D.W., Espenshade, G.H., and Shaw, K.W., 1973, Stratigraphy and structure of the metamorphic belt in northwestern North Carolina and southwestern Virginia: A study from the Blue Ridge across the Brevard Zone to the Sauratown Mountains anticlinorium: Amer. Jour. Sci., v. 273-A, p. 1-40.

Rankin, S.W., Stern, T.W., McLelland, J., Zartman, R.E., and Odom, A. L., 1983, Correlation chart for Precambrian rocks of the eastern United States: U.S. Geol. Survey Prof. Paper 1291-E, p. E1-E18.

Raymond, L.A., and Swanson, S.E., 1981, Deformation history of ultramafic rocks, Blue Ridge Belt, southern Appalachian Mountain,m Correlations with Appalachian tectonic events [abs]: Geol. Soc. Amer. Abs. with Programs, v. 13, p. 535.

Robinson, P., Spear, F.S., Schumacher, J.C., Laird, J., Klein, C., Evans, B.W., and Doolan, B.L., 1982, Phase relations of metamorphic amphiboles: natural occurrence and theory in Veblen, D.R., and Ribbe, P.H., eds., Amphiboles: Petrology and experimental phase relations, Mineralogical Society of America, Reviews in mineralogy, v. 9B, 390p.

Rock, N.M.S., Macdonald, R., Walker, B.H., May, F., Peacock, J.D., and Scott, P., 1985, Intrusive metabasite belts within the Moine assemblage west of Loch Ness, Scotland: evidence for metabasite modification by country rock interactions: Jour. Geol. Soc. London, v. 142, p. 643-661.

Shervais, J.W., 1982, Ti-V plots and the petrogenesis of modern and ophiolitic lavas: Earth and Planet. Sci. Lett., v. 59, p. 101-118.

Spear, F.S., 1981, Amphibole-plagioclase equilibria: An empirical model for the relation albite + tremolite = edenite + 4quartz: Contr. Min. Pet., v. 77, p. 355-364.

Stephenson, N.C.N., 1980, Precambrian amphibolites and basic granulites of the south coast of western Australia: Jour. Geol. Soc. Aust., v. 27, p. 91-104.

Stevens, R.K., Strong, D.F., and Keane, B.F., 1974, Do some eastern Appalachian ultramafic rocks represent mantle diapirs produced above a subduction zone?: Geology, v. 2, p. 175-178.

Stowe, S.H., Neilsen, M.J., and Neathery, T.L., 1984, Petrography, geochemistry and tectonic significance of the amphibolites of the Alabama Piedmont: Amer. Jour. Sci., v. 284, p. 416-436.

Sun, S., and Nesbitt, R.W., 1978, Geochemical regularities and genetic significance of ophiolitic basalts: Geology, v. 6, p. 689-693.

Swanson, S.E., 1980, Petrology of the Rich Mountain ultramafic bodies and associated rocks, Watauga County, North Carolina: Southeastern Geology, v. 21, no. 3, p. 25-48.

Thompson, G., 1978, A Geochemical study of the low temperature interaction of sea water and oceanic igneous rocks: Eos, v. , p. .

Thompson, R.N., Dickin, A.P., Gibson, I.L., and Morrison, M.A., 1982, Elemental fingerprints of isotopic contamination of Hebrdean Paleocene mantle-derived magmas by Archean Sial: Cont. Min. Pet., v. 79, p. 159-168.

Vincent, H.B., Jr., 1983, Metamorphosed mafic dikes within the Cranberry Gneiss and their relation to amphibolites of the Ashe Formaiton: North Carolina-Tennessee Blue Ridge [abs]: Geol. Soc. Amer. Abs. with Program, v. 15, p. 51.

Wehr, F., and Glover, L.,1985, Stratigraphy and tectonics of the Virginia-North Carolina Blue Ride: Evolution of a late Proterozoic hinge zone: Geol. Soc. America Bull., v. 96, p. 285-295.

Weigland, P.W., and Ragland, P.C., 1970, Geochemistry of Mesozoic dolerite dikes of eastern North America: Contr. Min. Pet., v. 29, p. 195-214.

Wilband, J.T., and Wasuwanich, P., 1980, Models of basalt petrogenesis: Lower Keweenawan Portage Lakes Lavas, Upper Michigan: Contr. Min. Pet., v. 75, p. 395-406.

APPENDICES

APPENDIX A

X-ray Fluorescence Procedures

APPENDIX A

Because this is one of the first studies from the University of Tennessee to utilize the new, automated x-ray fluorescence apparatus, it is desirable to briefly summarize methods used to develop the program used for chemical analyses of igneous rocks.

Spectra for the oxides Na_2O, MgO, Al_2O_3, SiO_2, P_2O_5, K_2O, CaO, MnO, Fe_2O_3, TiO_2 and the elements Cr, Ni, Rb, Sr, V, Y, Zr and Nb were gathered from 22 standards. These standards are from various geologic institutions such as the U.S.G.S. and the South Africa Bureau of Mines and Standards. Table A-1 gives a list of standards used and their respective rock types. A wide variety of standards was used so that a wide range of rock types could be analyzed.

NORM1 is a piece of glass, prepared especially for use as a normalization standard. Interelement corrections were done for all elements and these greatly lowered the standard error of calibration. One to three standards were removed for each element during interelement corrections and these were generally picked automatically by the computer. The Beers equation was used for all interelement corrections with the exception of CaO, which was stripped from phosphorous, and Ti which was stripped from vanadium.

Although the program used for this study is reasonably accurate and precise for most elements, several refinements are possible. The only element of the 18 that were analyzed which is not usable is Cr. Because all standards except SARM8 were made using a tungsten carbide grinding mill, Cr values are anomalously high. This problem may be rectified by two methods. The first would require making new standards and then redoing the entire program. Another technique would be to enter a region if interest for W and then use that element during interelement corrections for Cr. At this time preliminary work has been done for using the second method.

Another problem that arose during interelement corrections was the effect of excess Sr which was injected into NORM1. This element was placed in the glass so that the five elements with atomic numbers close to 38 could all be normalized to the value for Sr. Unfortunately this created anomalously high values for Y such that when Y was used as an interfering element for Sr and Zr, its effect was overestimated. Y was estimated to have an effect on the order of 10^{30}%, thus causing the protocol program to "bomb". Therefore Y could not be used as an interfering element. Although Zr values are relatively accurate and precise, they are consistently low. This may be caused by Y acting as an absorber. To remedy this problem, a program should be constructed that does not use NORM1.

However, because NORM1 simplifies the normalization procedure done before each run, it is desirable to use it for all elements except Rb, Sr, Y, Zr and Nb. Thus, the long term goal for efficient whole-rock analyses should be the creation of at least two and possibly three different protocols, one for major elements and transition metals, and one for trace elements.

Standards used for IGROCK (XRF) protocol.

AGV-1	Andesite	PCC-1	Dunite
BCR-1	Basalt	RGM-1	Rhyolite
BHVO-1	Basalt	SARM3	Lujavrite
BIR-1	Basalt	SARM4	Norite
DKBM	Basalt	SARM5	Pyroxenite
DNC-1	Dunite	SARM6D	Dunite
DTS-1	Dunite	SARM8	Chromium Ore
G2	Granite	SRM98A	Plastic Clay
GSP-1	Granite	SRM688	Basalt
MRG-1	Gabbro	STM-1	Nepheline Syenite
NORM1	Glass	W-2	Diabase

Values for selected standards (value in parentheses represent number of replicate analyses).

AGV-1 (20)

Element	Std. Value	Mean	Std Dev	Std Error Cal.
Na2O	4.26	4.19	0.13	0.16
MgO	1.53	1.54	0.1	0.23
Al2O3	17.25	17.28	0.29	0.27
SiO2	59	59.19	0.27	0.73
P2O5	0.49	0.486	0.022	0.04
K2O	2.89	2.92	0.038	0.07
CaO	4.9	4.89	0.055	0.09
MnO	0.097	0.099	0.004	0.03
Fe2O3	6.76	6.75	0.126	0.2
TiO2	1.04	1.07	0.02	0.03
V	125	114	8.8	0.003
Cr	12	6.2	7.3	0.006
Ni	19	21.3	6.5	0.003
Rb	67	63	5.6	0.0005
Sr	657	701	18.9	0.004
Y	21	21.8	2	0.0005
Zr	225	215	9	0.002
Nb	15	13.8	1.7	0.0003

G-2 (6)

Element	Std Value	Mean	Std Dev	Std Error Cal.
Na2O	4.07	4.23	0.1	0.16
MgO	0.76	0.86	0.03	0.23
Al2O3	15.4	15.58	0.1	0.27
SiO2	69.11	69.45	0.19	0.73
P2O5	0.14	0.12	0.009	0.04
K2O	4.51	4.45	0.04	0.07
CaO	1.94	2	0.004	0.09
MnO	0.034	0.043	0.001	0.03
Fe2O3	2.65	2.68	0.008	0.2
TiO2	0.5	0.49	0.01	0.03
V	35	44	0.82	0.003
Cr	7	n.d.		0.006
Ni	5	9	2.9	0.003
Rb	168	159	3.16	0.0005
Sr	479	486	8.1	0.004
Y	12	20	1.2	0.0005
Zr	300	303	14	0.002
Nb	14	16	1	0.0003

BCR-1 (10)

Element	Std Value	Mean	Std Dev	Std Error Cal.
Na2O	3.27	3.34	0.17	0.16
MgO	3.46	3.41	0.15	0.23
Al2O3	13.61	13.65	0.3	0.27
SiO2	54.5	55.04	0.36	0.73
P2O5	0.36	0.35	0.01	0.04
K2O	1.7	1.7	0.01	0.07
CaO	6.92	6.84	0.03	0.09
MnO	0.18	0.2	0.01	0.03
Fe2O3	13.4	13.13	0.05	0.2
TiO2	2.2	2.16	0.02	0.03
V	399	263	11	0.003
Cr	18	191	16	0.006
Ni	16	45	9	0.003
Rb	47	40	3.5	0.0005
Sr	330	290	8	0.004
Y	37	32	2.5	0.0005
Zr	190	150	3	0.002
Nb	14	14.5	2	0.0003

APPENDIX B

Whole Rock Analyses of Amphibolites

Whole rock analyses of amphibolite samples (oxides in wt%; elements in ppm).

Sample #	As-4	As-12	As-14	As-17	As-27
Na2O	2.16	2.92	2.84	3.23	2.34
MgO	5.59	6.13	5.31	7.99	5.54
Al2O3	14.05	12.88	11.80	13.82	12.01
SiO2	55.71	47.89	54.27	48.06	50.79
P2O5	1.05	0.44	0.38	0.16	0.43
K2O	0.55	0.27	0.21	0.19	0.82
CaO	6.44	9.79	9.12	8.88	9.24
MnO	0.18	0.21	0.22	0.22	0.22
TiO2	3.25	3.23	3.43	2.26	3.16
V	178.00	315.00	292.00	329.00	296.00
Cr	221.00	330.00	310.00	229.00	221.00
Fe2O3*	13.08	16.44	13.60	15.39	16.06
Ni	48.00	93.00	69.20	98.00	61.00
Rb	11.00	2.00	1.30	9.70	12.70
Sr	123.00	140.00	214.00	192.00	168.00
Y	43.80	39.00	52.40	25.00	42.80
Zr	296.00	187.00	208.00	132.00	209.00
Nb	27.20	13.60	15.20	12.30	21.00
Total	102.87	100.31	101.29	100.29	100.70
Ti/V	109.00	61.47	70.42	41.18	64.00
Zr/P2O5	281.90	421.17	545.93	809.82	488.32
Mg#	43.14	39.83	40.93	47.96	37.98
Y/Nb	1.61	2.87	3.45	2.03	2.04
Zr/Nb	10.88	13.75	13.68	10.73	9.95
Zr/Y	6.76	4.79	3.97	5.28	4.88
Nb/Y	0.62	0.35	0.29	0.49	0.49

As-36	As-62	As-66	As-96	AB-3	AB-4
2.96	1.28	2.25	2.58	2.57	1.78
6.23	5.60	4.31	6.75	6.31	5.24
14.31	12.06	13.78	12.93	14.31	13.44
49.28	49.72	50.93	49.13	45.54	49.21
0.24	0.29	0.84	0.34	0.41	0.40
0.25	0.27	2.39	0.26	0.98	1.01
9.59	11.22	6.76	9.25	9.60	8.52
0.19	0.21	0.20	0.25	0.33	0.22
2.87	2.82	3.40	3.02	3.15	3.05
302.00	394.00	191.00	334.00	317.00	279.00
209.00	306.00	190.00	327.00	265.00	245.00
14.29	16.72	15.03	16.93	18.30	16.66
65.00	89.20	29.00	103.00	79.00	61.00
4.20	0.60	37.00	1.90	13.00	11.50
202.00	162.00	255.00	102.00	232.00	145.00
23.90	35.80	40.00	32.70	41.80	51.60
149.00	153.00	259.00	161.00	221.00	223.00
10.40	13.50	32.00	15.60	18.50	21.50
100.31	100.29	99.97	101.53	101.62	99.62
56.97	42.91	106.72	54.21	59.57	65.54
623.43	525.77	308.70	476.33	536.41	564.56
43.63	37.28	33.73	41.44	37.97	35.83
2.30	2.65	1.25	2.10	2.26	2.40
14.33	11.33	8.09	10.32	11.95	10.37
6.23	4.27	6.48	4.92	5.29	4.32
0.44	0.38	0.80	0.48	0.44	0.42

Ab-5	AB-8	AB-17	As-9	As-20	As-24
1.90	2.04	2.23	2.55	1.28	1.51
5.69	5.01	5.66	7.02	8.83	7.95
13.15	13.81	13.45	12.85	12.28	12.07
50.04	50.24	49.52	47.68	51.69	50.67
0.39	0.39	0.51	0.07	0.02	0.06
0.97	0.92	0.35	0.17	0.19	0.17
8.13	8.17	11.01	9.61	11.64	11.13
0.23	0.21	0.18	0.22	0.15	0.18
3.06	3.13	2.85	0.74	0.15	0.44
258.00	249.00	321.00	445.00	290.00	356.00
247.00	224.00	178.00	299.00	217.00	175.00
16.66	16.56	15.41	17.59	12.89	14.88
68.00	68.00	58.00	127.00	85.00	95.00
12.70	12.00	3.30	2.90	5.50	3.30
228.00	276.00	251.00	38.00	54.00	30.00
42.00	36.00	39.80	28.70	4.10	18.60
226.00	198.00	195.00	31.00	11.00	13.00
21.90	16.10	14.90	2.90	0.10	0.10
100.32	100.96	101.27	98.58	99.18	99.13
71.10	75.36	53.23	9.97	3.10	7.41
575.06	506.39	380.12	436.62	728.48	203.13
37.74	34.94	39.47	41.47	54.87	48.67
1.92	2.24	2.67	9.90	41.00	186.00
10.32	12.30	13.09	10.69	110.00	130.00
5.38	5.50	4.90	1.08	2.68	0.70
0.52	0.45	0.37	0.10	0.02	0.01

As-29	As-37	As-52	As-53	As-58	As-61
2.99	1.55	1.60	1.25	1.14	1.31
7.36	7.96	7.03	8.43	5.95	8.62
13.50	12.13	12.62	12.23	11.51	11.47
48.09	49.97	51.66	51.26	52.83	50.86
0.05	0.08	0.02	0.02	0.04	0.02
0.32	0.13	0.16	0.12	0.08	0.10
9.88	11.55	10.48	11.94	10.36	13.99
0.19	0.20	0.15	0.18	0.20	0.16
0.54	0.89	0.35	0.17	0.23	0.21
368.00	417.00	378.00	304.00	406.00	346.00
310.00	210.00	219.00	118.00	245.00	190.00
15.90	14.76	14.42	13.28	16.27	12.18
127.00	79.00	99.00	86.00	107.00	80.00
4.80	1.60	3.40	0.10	1.90	2.10
27.70	53.00	32.00	29.00	31.00	33.00
19.20	27.80	12.20	6.40	6.00	6.40
20.00	43.00	20.00	10.00	10.00	15.00
1.60	0.90	0.10	0.10	0.10	0.10
98.91	99.31	98.58	98.93	98.69	99.00
8.80	12.80	5.55	3.35	3.40	3.64
384.62	558.44	1000.00	500.00	256.41	882.35
45.10	48.91	46.39	52.98	39.36	55.68
12.00	30.89	122.00	64.00	60.00	64.00
12.50	47.78	200.00	100.00	100.00	150.00
1.04	1.55	1.64	1.56	1.67	2.34
0.08	0.03	0.01	0.02	0.02	0.02

As-63	As-64	As-69	As-71	As-76	As-92
2.35	2.24	0.91	1.63	2.36	1.74
7.38	6.39	5.75	9.91	7.89	8.00
12.79	12.56	12.94	11.81	13.30	12.58
49.44	49.50	51.19	47.46	44.89	50.69
0.09	0.12	0.29	.00	0.18	0.08
0.23	0.13	0.18	0.30	0.13	0.25
10.44	11.10	15.86	12.67	10.91	11.95
0.16	0.21	0.14	0.20	0.22	0.17
0.96	1.03	0.85	0.39	1.30	0.42
385.00	432.00	490.00	392.00	432.00	365.00
234.00	184.00	121.00	636.00	443.00	248.00
15.21	16.34	12.78	14.92	18.07	13.55
82.00	84.00	26.90	161.00	96.00	92.00
6.10	1.30	1.10	6.90	8.10	2.50
67.00	57.00	287.00	44.00	43.80	73.00
30.00	27.70	19.70	10.70	37.10	14.30
46.00	45.00	71.00	24.00	70.00	35.00
0.50	0.50	0.10	0.10	7.00	0.10
99.14	99.70	101.00	99.43	99.35	99.51
14.95	14.29	10.40	5.96	18.04	6.90
541.18	387.93	246.53	6000.00	395.48	420.67
46.27	40.97	44.40	54.11	43.66	51.17
60.00	55.40	197.00	107.00	5.30	143.00
92.00	90.00	710.00	240.00	10.00	350.00
1.53	1.62	3.60	2.24	1.89	2.45
0.02	0.02	0.01	0.01	0.19	0.01

As-5	As-6	As-7	As-8	As-10	As-15
3.23	3.53	4.47	3.53	0.47	3.19
7.40	5.67	6.05	7.80	28.33	6.38
17.71	15.21	15.67	15.88	7.62	15.25
50.21	49.81	50.94	48.03	43.09	47.87
0.21	0.30	0.36	0.33	0.14	0.41
0.15	0.67	0.20	0.82	0.00	1.68
10.97	9.92	8.33	10.24	4.03	10.25
0.10	0.18	0.17	0.15	0.22	0.18
1.02	1.55	1.80	2.02	0.55	1.56
227.00	276.00	247.00	280.00	132.00	373.00
186.00	93.00	41.00	40.00	2520.00	113.00
8.42	11.69	11.08	9.36	13.47	12.88
57.00	23.00	19.00	41.00	1050.00	13.00
6.80	6.50	5.00	41.00	6.40	27.00
332.00	341.00	299.00	250.00	28.00	612.00
22.20	23.50	32.50	32.00	17.40	16.90
136.00	172.00	189.00	173.00	52.00	113.00
2.00	12.60	17.60	11.80	6.00	8.40
99.50	98.63	99.15	98.23	98.28	99.75
26.94	33.67	43.69	43.25	24.75	25.07
647.62	579.12	519.23	517.96	363.64	278.33
60.94	46.26	49.22	59.66	78.87	46.79
11.10	1.87	1.85	2.71	2.90	2.01
68.00	13.65	10.74	14.66	8.67	13.45
6.13	7.32	5.82	5.41	2.99	6.69
0.09	0.54	0.54	0.37	0.34	0.50

As-22	As-31	As-32	As-39	As-40	As-43
3.04	2.04	2.72	3.39	2.58	2.35
9.98	7.38	8.21	9.86	7.20	7.40
13.68	12.89	13.44	15.08	13.98	13.93
49.97	52.14	50.04	46.92	48.32	49.61
0.08	0.16	0.15	0.16	0.27	0.15
0.09	0.43	0.15	0.16	0.39	0.28
7.12	11.00	10.18	6.64	10.75	10.56
0.17	0.17	0.19	0.19	0.19	0.19
0.75	1.24	1.84	1.32	1.78	1.26
266.00	315.00	307.00	219.00	330.00	319.00
473.00	282.00	170.00	141.00	256.00	82.00
13.14	11.88	12.48	12.64	14.03	12.87
126.00	85.00	60.00	64.00	55.00	42.00
4.80	7.80	6.20	2.20	10.00	7.20
90.00	173.00	88.00	73.00	97.00	98.00
29.40	33.00	24.80	35.70	42.00	32.90
42.00	132.00	94.00	97.00	105.00	94.00
5.80	6.40	7.00	10.40	10.20	1.70
98.12	99.42	99.46	96.42	99.68	98.66
16.90	23.60	35.93	36.13	32.34	23.68
560.00	809.82	618.42	613.92	396.23	643.84
57.41	52.44	53.87	58.06	47.67	50.51
5.07	5.16	3.54	3.43	4.12	19.35
7.24	20.63	13.43	9.33	10.29	55.29
1.43	4.00	3.79	2.72	2.50	2.86
0.20	0.19	0.28	0.29	0.24	0.05

As-45	As-47	As-49	As-56	As-65	As-67
2.81	2.73	3.61	2.87	2.09	1.43
6.52	7.05	7.35	6.68	8.55	8.21
15.94	14.27	16.20	13.93	13.48	14.20
49.10	49.51	49.31	49.85	47.64	49.48
0.16	0.16	0.17	0.33	0.18	0.15
0.44	0.26	0.25	0.31	0.41	0.32
10.37	10.00	9.38	10.03	12.09	11.59
0.17	0.19	0.16	0.20	0.17	0.28
1.36	1.40	1.29	1.88	1.19	1.33
290.00	315.00	245.00	312.00	353.00	361.00
140.00	95.00	157.00	221.00	218.00	186.00
11.72	13.25	10.66	14.15	13.48	13.36
52.00	42.00	45.00	50.00	42.50	46.00
6.70	2.40	4.40	3.20	11.10	3.20
137.00	117.00	157.00	100.00	125.00	95.00
35.70	35.00	34.00	51.00	31.10	33.30
105.00	98.00	102.00	148.00	85.00	85.00
4.80	3.40	1.80	13.70	4.80	1.80
98.66	98.89	98.45	100.31	99.38	100.42
28.11	26.64	31.57	36.12	20.21	22.09
640.24	628.21	618.18	445.78	461.96	566.67
49.68	48.57	55.03	45.59	52.96	52.17
7.44	10.29	18.89	3.72	6.48	18.50
21.88	28.82	56.67	10.80	17.71	47.22
2.94	2.80	3.00	2.90	2.73	2.55
0.13	0.10	0.05	0.27	0.15	0.05

As-68	As-73	As-74	As-77	As-80	As-81
2.27	2.55	3.59	2.46	3.04	2.74
7.88	8.35	5.32	7.32	8.63	7.71
15.42	14.61	17.08	14.37	15.28	15.15
47.86	49.72	51.98	51.86	48.68	48.61
0.11	0.10	0.22	0.15	0.25	0.21
0.47	1.23	0.86	0.11	0.22	0.49
11.91	10.82	7.72	8.11	9.75	10.52
0.19	0.15	0.10	0.28	0.21	0.15
1.49	0.94	1.12	1.25	1.24	1.40
317.00	288.00	181.00	207.00	246.00	284.00
231.00	216.00	168.00	233.00	189.00	297.00
12.20	10.32	9.64	13.49	11.98	12.28
67.00	67.00	45.00	63.00	110.00	89.00
7.30	38.60	29.00	5.40	4.80	9.60
168.00	175.00	214.00	143.00	129.00	168.00
42.80	23.70	34.10	33.70	44.20	33.70
184.00	70.00	131.00	123.00	94.00	110.00
10.80	1.00	7.30	8.70	5.00	4.60
99.89	98.86	97.73	99.48	99.34	99.36
28.18	19.50	37.10	36.20	30.22	29.55
1642.86	714.29	600.92	831.08	377.51	531.40
53.41	58.95	49.48	49.06	56.11	52.71
3.96	23.70	4.67	3.87	8.84	7.33
17.04	70.00	17.95	14.14	18.80	23.91
4.30	2.95	3.84	3.65	2.13	3.26
0.25	0.04	0.21	0.26	0.11	0.14

As-82	As-85	As-86	As-87	As-89	As-90
2.78	2.42	2.41	2.44	1.45	1.81
7.22	7.87	7.92	8.32	9.49	11.63
14.14	14.07	14.12	14.14	13.97	12.23
51.00	48.76	50.31	48.63	50.96	49.37
0.27	0.20	0.18	0.12	0.07	0.12
0.29	0.22	0.16	0.38	0.25	0.32
10.32	11.47	12.21	12.68	12.26	12.47
0.17	0.12	0.14	0.16	0.14	0.13
1.43	1.37	1.26	1.14	0.74	0.72
288.00	321.00	331.00	351.00	254.00	287.00
213.00	241.00	120.00	159.00	142.00	499.00
12.15	12.25	11.33	11.93	9.50	10.77
54.00	82.00	50.00	57.00	41.00	126.00
5.30	7.80	8.20	8.00	3.90	9.60
164.00	120.00	169.00	126.00	163.00	112.00
33.20	34.90	27.10	26.90	26.40	15.10
122.00	95.00	101.00	88.00	66.00	70.00
7.20	0.40	1.50	2.60	0.10	0.10
99.85	98.82	100.11	100.01	98.90	99.69
29.77	25.59	22.82	19.47	17.47	15.04
458.65	484.69	551.91	715.45	916.67	593.22
51.33	53.28	55.37	55.32	63.94	65.72
4.61	87.25	18.07	10.35	264.00	151.00
16.94	237.50	67.33	33.85	660.00	700.00
3.67	2.72	3.73	3.27	2.50	4.64
0.22	0.01	0.06	0.10	.00	0.01

As-94	As-95	AB-1	AB-2	AB-7	AB-9
0.76	3.17	3.34	0.96	2.45	2.40
23.77	6.43	4.95	7.00	6.69	8.94
7.37	15.22	16.35	14.78	14.80	14.09
45.92	48.06	51.42	47.74	53.16	49.84
0.09	0.41	0.33	0.12	0.15	0.21
0.00	0.40	1.40	0.14	0.12	0.26
5.29	11.39	7.05	17.75	11.63	10.89
0.27	0.17	0.13	0.12	0.12	0.14
0.53	1.92	1.90	1.35	1.01	1.34
168.00	315.00	203.00	463.00	210.00	252.00
3920.00	125.00	241.00	170.00	230.00	300.00
13.11	12.93	12.27	11.07	9.44	11.35
837.00	46.00	85.00	28.70	66.00	97.00
5.50	7.90	41.00	4.60	1.70	3.70
40.00	267.00	450.00	299.00	188.00	163.00
12.00	23.90	32.80	21.40	22.00	28.10
54.20	140.00	266.00	127.00	95.00	118.00
6.80	15.20	21.60	4.30	3.80	10.00
97.56	100.17	99.26	101.12	99.66	99.57
18.84	36.54	56.11	17.48	28.83	31.88
618.02	345.68	810.98		641.89	556.60
76.29	46.88	41.73	52.88	55.71	58.30
1.76	1.57	1.52	4.98	5.79	2.81
7.97	9.21	12.31	29.53	25.00	11.80
4.52	5.86	8.11	5.93	4.32	4.20
0.57	0.64	0.66	0.20	0.17	0.36

AB-10	AB-11	AB-12	AB-13	AB-14	AB-15
2.96	3.58	1.00	2.49	3.58	2.65
6.81	6.67	4.71	7.97	6.74	8.77
14.90	14.68	16.54	17.54	16.91	13.30
50.31	50.95	48.75	45.79	49.33	47.85
0.17	0.21	0.15	0.20	0.17	0.17
0.15	0.32	0.13	0.83	0.26	0.53
12.23	10.69	17.96	11.55	11.38	12.78
0.14	0.16	0.12	0.15	0.14	0.17
1.28	1.33	1.19	1.38	1.15	1.26
294.00	255.00	464.00	261.00	255.00	299.00
239.00	293.00	167.00	270.00	226.00	210.00
10.46	10.89	11.11	11.47	10.10	10.56
64.00	84.00	41.00	78.00	58.00	76.00
5.20	4.60	2.90	22.00	6.00	13.20
210.00	121.00	267.00	164.00	164.00	163.00
23.20	28.90	17.70	26.90	24.60	22.50
120.00	115.00	113.00	117.00	108.00	103.00
7.00	8.00	4.70	7.00	6.00	8.10
99.52	99.57	101.75	99.45	99.83	98.13
26.10	31.27	15.38	31.70	27.04	25.26
701.75	539.91		593.91	627.91	595.38
53.61	52.09	42.94	55.22	54.22	59.58
3.31	3.61	3.77	3.84	4.10	2.78
17.14	14.38	24.04	16.71	18.00	12.72
5.17	3.98	6.38	4.35	4.39	4.58
0.30	0.28	0.27	0.26	0.24	0.36

AB-16

2.82
9.99
15.09
49.30
0.19
0.44
10.50
0.14
1.01
250.00
445.00
9.95
145.00
12.30
131.00
24.50
96.00
7.70
99.55

24.22
505.26
64.06
3.18
12.47
3.92
0.31

APPENDIX C

Representative Hornblende Analyses

Representative hornblende analyses*

	As-4	As-22
SiO2	44.7 (7)	45.3 (3)
Al2O3	14.9 (3)	14.5 (3)
TiO2	0.61(2)	0.46(2)
MgO	11.3 (2)	12.5 (2)
FeO	14.1 (2)	13.5 (2)
MnO	0.14(4)	0.21(3)
CaO	10.5 (2)	10.1 (1)
Na2O	1.70(1)	1.6 (1)
K2O	0.33(2)	0.22(2)
Total	98.28	98.39

Cation proportions normalized to:

	23 O	13 cations		
Si	6.38	6.25	6.42	6.27
Al IV	1.62	1.75	1.58	1.73
Al VI	1.12	0.94	1	0.79
Ti	0.06	0.06	0.05	0.05
Fe3+				
Mg	2.37	2.33	2.64	2.58
Fe2+	1.45	1.66	1.31	1.55
Mn		0.01		0.02
Fe2+	0.25		0.27	
Mn	0.01		0.02	
Ca	1.64	1.61	1.64	1.6
Na	0.1	0.39	0.07	0.4
Na	0.4	0.1	0.44	0.11
K	0.06	0.07	0.04	0.03
Ca				
Total	15.46	15.18	15.48	15.14
Total Charges	45.98	45.08	45.95	44.84

* Number in parentheses is 1 standard deviation in terms of last decimal cited.

AB-1	AB-15
43.9 (4)	48.0 (1.3)
14.1 (3)	10.2 (1.1)
0.89 (4)	0.4 (1)
8.6 (1)	14.5 (8)
17.7 (2)	11.9 (9)
0.17(2)	0.29(04)
11.1 (1)	11.4 (1)
1.5 (1)	1.6 (2)
0.71(4)	0.4 (1)
98.67	98.69

Cation proportions normalized to:

		23 O	13 cation
6.36	6.28	6.73	6.62
1.64	1.72	1.27	1.38
0.96	0.84	0.61	0.48
0.09	0.09	0.05	0.04
1.83	1.81	2.86	2.93
2.12	2.23	1.48	1.51
	0.03		0.04
0.13		0.05	
0.02		0.04	
1.81	1.8	1.78	1.75
0.04	0.2	0.13	0.25
0.4	0.23	0.33	0.19
0.145	0.14	0.07	0.07
15.54	15.37	15.4	15.26
46	45.47	45.71	45.19

APPENDIX D

Other Representative Analyses

Representative analyses of other minerals

Plagioclase

	As-4	As-22	AB-1	AB-15
SiO2	60.0 (4)	60.4 (6)	59.7 (5)	62.7 (4)
Al2O3	26.1 (2)	25.6 (2)	25.6 (3)	23.3 (1)
CaO	6.90(2)	5.70(2)	7.30(3)	4.70(1)
Na2O	7.60(3)	8.10(4)	7.50(5)	8.90(2)
K2O	n.d.	n.d.	n.d.	n.d.
Total	100.60	99.80	100.10	99.60
Cations normalized to 8 O				
Si	2.65	2.68	2.66	2.78
Al	1.36	1.34	1.34	1.22
Ca	0.33	0.27	0.35	0.22
Na	0.65	0.70	0.64	0.77
K	n.d.	n.d.	n.d.	n.d.
Total	4.99	4.99	4.99	4.99

Garnet

Sample	As-4	As-4	As-22	As-22	AB-1	AB-1
	Rim	Core	Rim	Core	Rim	Core
SiO2	37.27	38.55	37.75	37.62	37.14	36.95
Al2O3	21.71	21.32	21.79	21.40	21.77	21.61
FeO	30.58	29.32	29.66	28.30	29.96	30.35
MgO	4.64	4.64	4.36	3.15	2.93	2.84
CaO	4.73	4.90	4.94	7.38	5.73	5.50
MnO	0.95	1.01	1.70	2.36	2.71	2.78
Total	100.05	99.44	100.25	100.37	100.32	100.16
Cations normalized to 12 O						
Si	2.95	3.01	2.98	2.98	2.95	2.95
Al	2.03	1.99	2.03	2.00	2.04	2.03
Fe	2.02	1.94	1.96	1.87	1.99	2.03
Mg	0.55	0.55	0.51	0.37	0.35	0.34
Ca	0.40	0.42	0.42	0.63	0.49	0.47
Mn	0.06	0.07	0.11	0.16	0.18	0.19
Total	8.02	7.97	8.00	8.01	8.01	8.01
Alm	0.75	0.74	0.73	0.69	0.72	0.73
Py	0.11	0.12	0.11	0.08	0.07	0.07
Gr	0.12	0.12	0.12	0.18	0.14	0.13
Sp	0.02	0.03	0.04	0.06	0.07	0.07

	Ilmenite	
Samples	As-4	As-22
FeO	46.6 (3)	45.5 (3)
TiO2	52.4 (3)	52.4 (3)
MnO	0.30(1)	1.60(1)
MgO	0.50(1)	0.10(02)
Al2O3	0.11(02)	0.20(01)
Total	99.91	99.83
Fe	0.98	0.96
Ti	0.99	0.99
Mn	0.01	0.04
Mg	0.02	n.d.
Al	0.01	0.01
Total	2.00	2.00

Cum ingtonite

As-22

SiO2	55.0 (4)
Al2O3	0.91(04)
MgO	20.6 (3)
FeO	21.6 (3)
MnO	0.35(2)
CaO	0.6 (1)
Total	99.30

Cations normalized to 23 O

Si	7.83
Al	0.15
Mg	4.38
Fe3+	
Fe2+	2.57
Mn	0.04
Ca	0.09
Total	15.09
Charges	45.92
Fe3+	0.08

Biotite

AB-1

SiO2	35.6 (1)
Al2O3	16.9 (1)
MgO	10.4 (1)
TiO2	1.90(1)
K2O	9.30(1)
FeO	20.5 (2)
MnO	0.13(01)
Total	94.73

Cations normalized to 22 O

Si	5.49
Al	3.07
Mg	2.39
Ti	0.22
K	1.82
Fe	2.65
Mn	0.01
Total	15.64

Epidote

AB-15

SiO2	38.0 (1)
Al2O3	24.9 (3)
CaO	22.3 (1)
FeO	10.1 (3)
MnO	0.22(2)
Na2O	n.d.
Total	95.52

Cations normalized to 13 O

Si	3.24
Al	2.50
Ca	2.03
Fe	0.72
Mn	0.02
Na	n.d.
Total	8.51

APPENDIX E

Mineral Assemblages

Mineral assemblages for samples from Ashe and Alligator Back Formations

	hb	plg	gn	ep	qtz	bt	chl	opq	rut	sph	other
As-4	x	x	x		x			I			
As-5	x	x			x			I	x		
As-6	x	x		x	x	x				x	
As-7	x	x			x			I,P			
As-8	x	x			x	x	x	I,P	x	x	
As-9	x	x			x			I			
As-12	x	x			x			I			
As-14	x	x		x	x			I			
As-15	x	x			x						
As-17	x	x			x		x	I			
As-20	x	x			x						
As-22	x	x	x		x		x				cumm
As-24	x	x		x	x			I,M			
As-27	x	x			x	x		P		x	
As-29	x	x			x			I,C			
As-31	x	x		x	x			I	x	x	
As-32	x	x		x	x			P		x	
As-36	x	x			x					x	
As-37	x	x		x	x			I			
As-39	x	x			x		x	I	x		
As-40	x	x	x		x			I,H			
As-43	x	x			x			I		x	
As-45	x	x			x					x	
As-47	x	x			x			I			
As-49	x	x			x						
As-52	x	x		x	x			I			
As-53	x	x		x	x			I,H			
As-56	x	x	x		x						
As-58	x	x	x	x	x			I,H			
As-59	x	x			x		x				
As-61	x	x	x	x	x		x				cal
As-62	x	x		x	x			I	x		
As-63	x	x			x						
As-64	x	x		x	x			P,C		x	
As-65	x	x			x					x	
As-66	x	x	x		x	x					
As-67	x	x	x		x						

	hb	plg	gn	ep	qtz	bt	chl	opq	rut	sph	other
As-68	x	x		x	x					x	
As-69	x	x		x	x						
As-71	x	x		x	x						
As-73	x	x		x	x					x	
As-74	x	x			x			I,M	x		
As-76	x	x	x		x			I			
As-77	x	x	x		x			I			
As-80	x	x			x			I,H	x		
As-81	x	x			x					x	
As-82	x	x	x		x					x	
As-85	x	x			x					x	
As-86	x	x	x	x	x					x	
As-87	x	x			x						
As-89	x	x	x		x						
As-90	x	x	x		x						
As-91	x	x			x						
As-92	x	x			x						
As-95	x	x			x			I			
As-96	x	x			x			I			
AB-1	x	x	x	x	x	x		I,P			
AB-2	x	x		x	x						
AB-3	x	x		x	x		x	I			
AB-4	x	x		x	x		x	I			
AB-5	x	x		x	x		x	I		x	
AB-7	x	x		x	x	x		I	x		
AB-8	x	x		x	x			I			
AB-9	x	x		x	x						
AB-10	x	x		x	x						
AB-11	x	x		x	x			I			
AB-12	x	x		x	x			I			
AB-13	x	x		x	x			I			
AB-14	x	x		x	x	x	x	I			
AB-15	x	x		x	x		x	I	x		cal,ser
AB-16	x	x		x	x			I			ser
AB-17	x	x		x	x		x	I			

I (ilmenite), P (pyrite), C (chalcopyrite), H (hematite)
M (magnetite)

APPENDIX F

Abbreviations Used in Text

Abbreviations used in text.

As = Ashe Formation
A.B. = Alligator Back Formation
hnb = hornblende
plg = plag
qtz = quartz
ep = epidote
gar = garnet
bio = biotite
ilm = ilmenite
rut = rutile
sph = sphene
cal = calcite
cumm = cummingtonite
chl = chlorite
An = Anorthite
wpb = within-plate basalts
ofb = ocean floor basalts
MORB = mid-ocean ridge basalts
lkt = low potassium tholeiites
cab = calc-alkaline basalts
cfb = continental flood basalts

VITA

Jonathan Conte was born in Washington, Pennsylvania on November 18, 1961. After graduating from Trinity High School in 1979, he enrolled in Kenyon College, Gambier, Ohio. He transferred to the College of Wooster, Wooster Ohio, in the Fall of 1980 where he graduated with honors in June, 1983. During September of that year the entered the University of Tennessee, Knoxville, where he received a Master of Science degree in Geology in March, 1986.